



Feature Article

Polyelectrolyte complexes: Bulk phases and colloidal systems

Jasper van der Gucht*, Evan Spruijt, Marc Lemmers, Martien A. Cohen Stuart

Laboratory of Physical Chemistry and Colloid Science, Wageningen University, PO Box 8038, 6700 EK Wageningen, The Netherlands

ARTICLE INFO

Article history:

Received 10 February 2011

Accepted 28 May 2011

Available online 7 June 2011

Keywords:

Polyelectrolyte complexation

Phase behavior

Layer-by-layer assembly

Polyelectrolyte multilayers

Complex coacervate core micelles

ABSTRACT

When aqueous solutions of polycations and polyanions are mixed, polyelectrolyte complexes form. These are usually insoluble in water, so that they separate out as a new concentrated polymer phase, called a *complex coacervate*. The behavior of these complexes is reviewed, with emphasis on new measurements that shed light on their structural and mechanical properties, such as cohesive energy, interfacial tension, and viscoelasticity. It turns out that stoichiometric complexes can be considered in many respects as pseudo-neutral, weakly hydrophobic polymers, which are insoluble in water, but become progressively more soluble as salt is added. In fact, the solubility-enhancing effect of salt is quite analogous to that of temperature for polymers in apolar solvents.

Since two-phase systems can be prepared in colloidal form, we also discuss several kinds of colloids or 'microphases' that can arise due to polyelectrolyte complexation, such as thin films, 'zipper' brushes, micelles, and micellar networks. A characteristic feature of these charge-driven two-phase systems is that two polymeric ingredients are needed, but that some deviation from strict stoichiometry is tolerated. This turns out to nicely explain how and when the layer-by-layer method works, how a 'leverage rule' applies to the density of the 'zipper brush', and why soluble complexes or micelles appear in a certain window of composition. As variations on the theme, we discuss micelles with metal ions in the core, due to incorporation of supramolecular coordination polyelectrolytes, and micellar networks, which form a new kind of physical gels with unusual properties.

© 2011 Elsevier Inc. All rights reserved.

1. Introduction

Lyophobic colloids are biphasic systems, of which one phase is finely dispersed into the other. The very existence of such colloids is of course intimately related to the phase behavior of its constituents. In this article, we consider lyophobic colloids that have complexes of cationic and anionic macro-ions as their dispersed phase, in aqueous electrolyte as continuous phase. They are made by simply mixing solutions of the constituent macro-ions. In order to review colloidal properties, we first need to understand the phase behavior and the driving forces that underlie polyelectrolyte complex formation. We will focus on how molecular structure parameters (such as molar mass, charge density, and chemical groups), pH, and ionic strength influence the phase behavior. We then review

'microphases' based on electrostatic self-assembly, such as micelles, micro-emulsions, networks, and multilayers.

2. Phases of macro-ion complexes

2.1. Different kinds of macro-ion complexes

The most frequently studied kind of macro-ion complex is that between two oppositely charged polyelectrolytes. Many polyelectrolytes have high linear charge densities and are therefore likely to form strong complexes, which can be considered as archetypical for this class of materials [1–3]. In the case of weak polyacids or polybases, of which the degree of dissociation is pH dependent, complex formation occurs only in a limited pH range. A special case is hydroxypropyl guar (HPG), a non-ionic water-soluble polymer, which becomes anionic in the presence of borate ions that bind to the chain backbone. Because of the labile nature of this binding, the charge density responds to small changes in local conditions. Consequently, complex formation with a strong polycation stimulates further borate binding. This charge regulation causes the zeta potential of the complexes to be almost independent of the ratio between polycation and HPG [4]. Another somewhat unusual type of polyelectrolyte complex is that between a conventional polyelectrolyte and an oppositely charged supramolecular

Abbreviations: PDMAEMA, poly(2-(*N,N*-dimethyl amino)-ethyl methacrylate); PTMAEMA, poly(2-(*N,N,N*-trimethyl amino)-ethyl methacrylate); PEO, poly(ethylene oxide); P2MVP, poly(*N*-methyl-2-vinyl pyridinium iodide); PAA, poly(acrylic acid); PVA, poly(vinyl alcohol); PAAM, poly(acryl amide); PNIPAM, poly(*N*-isopropyl acrylamide); PSPMA, poly(3-sulfopropyl methacrylate); PSS, poly(styrene sulfonate); PEI, poly(ethylene imine); PAH, poly(allyl amine) hydrochloride; PDADMAC, poly(diallyldimethylammonium chloride); PMA, poly(maleic acid); PMMA, poly(methyl methacrylate); PLL, poly(L-lysine).

* Corresponding author. Fax: +31 317 483777.

E-mail address: jasper.vandergucht@wur.nl (J. van der Gucht).

polyelectrolyte. The latter component reversibly forms chain structures by means of weak, non-covalent bonds between small molecules; the prime example is a coordination polymer, with coordinated metals in the main chain that keep two organic ligands together [5].

Somewhat weaker complexes, but important in terms of application, are those between polyelectrolytes and proteins [6–17] or even between pairs of oppositely charged proteins [18]. Compaction of (anionic) DNA is driven by the formation of complexes with (cationic) proteins, such as histones [19–21]. Polyelectrolytes also tend to interact strongly with various small inorganic colloidal particles such as metal oxides or silica [22,23]. In a sense, such particles are also macro-ions, but their surfaces are amphoteric: they can bind and release protons and therefore carry both negative and positive charges, the net charge being dependent on the pH and the potential at the surface.

Finally, one could consider mixtures of oppositely charged colloidal particles, such as those studied by Van Blaaderen et al. [24,25] as macro-ion complexes; however, the more interesting ordered phases that appear for sufficiently weakly interacting particles are more comparable to salt crystals and will not be called ‘complexes’ in the present context.

Each of these classes of complexes has its special features. In this article, we focus mainly on complexes formed between linear polyelectrolyte chains or block copolymers with one or more polyelectrolyte blocks. Our discussion on the electrostatic driving forces and the phase behavior, however, applies also to the other classes of electrostatic complexes.

2.2. Thermodynamics of complex formation

Macro-ions in aqueous solution are surrounded by an electrical double layer: a zone with an increased concentration of counterions and a reduced concentration of co-ions. As compared to the (hypothetical) situation of complete random mixing, the double layer has lower energy (the average distance between positive and negative charges is smaller than that between positives or between negatives), but also lower entropy (small ions have less translational freedom). When two oppositely charged macro-ions form a complex, the double layers are destroyed to a certain extent and the counterions are released in the form of an ordinary salt solution (see Fig. 1). This implies changes in both the energy (enthalpy) and the entropy of the system. Both contributions will vary with the concentration of salt (ionic strength).

The entropy change associated with complex formation is likely to be positive; the release of counterions initially confined to a

double layer is the dominating term here. At low ionic strength, one expects a large contribution, as the ion concentrations inside the counterion clouds are significantly higher than that in the surrounding salt solution. As the salt concentration in the solution increases, the entropy gain for released counterions becomes smaller. This is indeed observed in computer simulations [26]. Another contribution to the entropy change is the loss of configurational and translational entropy of the polyelectrolyte chains upon complex formation. This term opposes complex formation, but for long chains, it is small compared with the counterion entropy, so that complexation is usually favored entropically.

It is easy to see that complexation may be either exothermic or endothermic, depending on salt concentration (see Fig. 2). At low salt concentration, the Debye screening length is large and the counterion clouds of the separate macro-ions are dilute, while the polyelectrolyte complexes are dense with tight ion pairing between oppositely charged groups. As a result, the electrostatic energy of the system decreases considerably upon complex formation, i.e., complexation is exothermic. At high salt concentrations, however, counterion clouds are compact, and the increase in energy due to the released ions is not compensated by the decrease in energy coming from the newly formed interpolyelectrolyte ion pairs, so that complexation is endothermic. This is confirmed by calorimetric data measured and collected by Schaaf et al. [27] and by Hofs et al. [28] As shown by computer simulations [26], the complexation energy also depends on the linear charge density of the polyelectrolytes. For weakly charged polyelectrolytes, complexation is exothermic, but for highly charged chains, it is endothermic, because a large fraction of the counterions is already strongly bound (condensed) to the chain before complexation.

The fact that the counterion entropy always favors complexation implies that complexation with a positive enthalpy is possible (and indeed occurs) at higher salt concentrations [27] (see Fig. 2). The salt concentration where crossover between exothermic and endothermic complexation occurs can vary significantly, depending on the polyelectrolyte pair chosen. This is probably due to variations in the charge density or in the ion pair energy, but possibly also dependent on the dielectric environment around an ion pair, hence on the chemical structure of the participating polyelectrolytes. Other factors such as Van der Waals forces, hydrophobic interactions, or hydrogen bonding may also contribute [29]. No clear understanding has been obtained here so far. An interesting observation is that the crossover between endothermic and exothermic complexation often seems to occur in the neighborhood of a change in mechanical behavior from solid-like to more liquid-like [27].

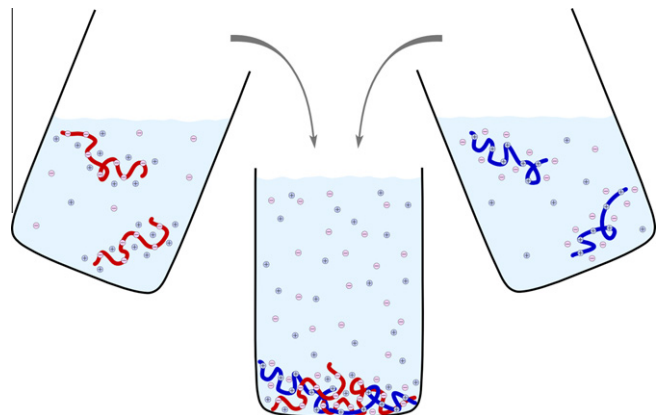


Fig. 1. Mixing solutions of polycations and polyanions can lead to associative phase separation and the formation of a polyelectrolyte complex phase.

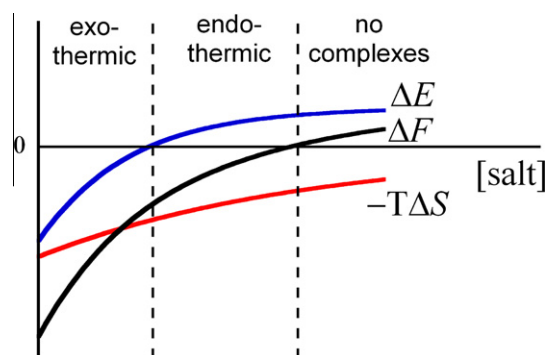


Fig. 2. Schematic picture showing the effect of salt on the total free energy of complexation (ΔF) and on the separate contributions of the counterion release entropy ($-T\Delta S$) and the Coulomb energy (ΔE). Complexation can be exothermic or endothermic, depending on the salt concentration.

An intriguing finding is that some complexes are very hard to dissolve in aqueous salt solutions, but dissolve readily in water/acetone mixtures containing certain dissolved salts, e.g. sodium bromide. This was found by Michaels et al. [30] and used for casting thin films of polyelectrolyte complexes: upon washing with water, an insoluble complex film was formed that could be used for filtration purposes. The solubility in acetone and the effect of anions have not been explained in a satisfactory manner.

Under conditions where the driving force for complex formation is very large, i.e. for strongly charged chains at low salt concentrations, the thermodynamic equilibrium state may not be easily reached. The ion pairing between ionic groups of the oppositely charged chains can be so strong that ion pairs never dissociate again once they are formed. This is quite common for highly charged polyelectrolytes at low or moderate ionic strengths and leads to quenched, non-equilibrium complexes. The final structure of these complexes depends strongly on the method of sample preparation, for example, on the order in which the polymers are mixed [31–35]. Below, in Section 3, we will discuss how the formation of polyelectrolyte multilayers and certain colloidal phases relies crucially on the fact that non-equilibrium complex states can be metastable.

2.3. Theory of polyelectrolyte complexation

The great problem in developing a theory of macro-ion complex formation is to find an accurate estimate of the electrostatic free energy. This free energy is determined by the spatial correlations between the various ionic groups, which are still poorly characterized.

The first theoretical treatment of polyelectrolyte complexation was that of Overbeek and Voorn [36], who estimated the total free energy as a sum of mixing entropy terms and an electrostatic contribution that is just the classical Debye–Hückel expression for a simple electrolyte solution. The former favors homogenous mixing, while the latter favors the formation of a dense complex phase. Phase diagrams calculated using the Voorn–Overbeek theory are discussed below. The Voorn–Overbeek theory has several serious limitations. For example, the random mixing approximation used for the distribution of ions neglects counterion condensation and double layer formation around the polyelectrolyte chains in the dilute phase. It therefore does not account for the entropy gain of the released counterions in a proper way. Another approximation in the Voorn–Overbeek theory is that it neglects the connectivity of the charges on the polyelectrolyte chains. For weakly correlated phases, this can be improved by using a random phase approximation that explicitly accounts for chain connectivity [37–39] or by loop expansions that go beyond the level of random phase approximation [40]. These models are limited to relatively weak charge correlations and therefore to polyelectrolytes of low charge density. A model that should apply to more strongly charged systems and that gives a better account of the contribution of counterions is the model of Biesheuvel and Cohen Stuart [41,42]. In this model, cylindrical cells are assumed around each polyelectrolyte chain, and the distribution of salt ions around the chains is found by solving the Poisson–Boltzmann equation. For very dense complex phases, the Poisson–Boltzmann equation, which treats the distribution of small ions as a smeared out continuous function, is no longer valid. Currently, there is no theory that gives a good description of the ion pairs in such strongly correlated phases. Langevin dynamics [26], molecular dynamics [43,44], and Monte Carlo [45–48] simulations have been performed on such strong complexes, but so far, no simulated phase diagrams have been presented. One other aspect that is not considered in the approaches mentioned above is the influence of smaller soluble complexes on the phase diagram. To account for this, Veis and Aranyi considered complex formation as a two-step process [49,50]. First,

spontaneous aggregation of oppositely charged chains takes place, driven by electrostatic interactions. The small aggregates formed in this way then rearrange to form a macroscopic concentrated coacervate phase. This second process is driven by an increase in configurational entropy. For conditions where one of the two polyelectrolytes is present in excess, this rearrangement is hindered by the excess charge on the aggregates, so that soluble complexes could be favored over macroscopic phase separation [51].

2.4. Phase diagram

A crucial descriptor of polyelectrolyte complex phases is the phase diagram. In the general case, we are dealing with a four-component system: a polycationic salt, a polyanionic salt, simple electrolyte, and water. In Fig. 3, we present a phase diagram calculated using the theory of Overbeek and Voorn [36] for a system consisting of polycations P and polyanions Q , each consisting of 100 charged segments, in the presence of monovalent salt. Although the Voorn–Overbeek theory makes debatable approximations for calculating the electrostatic free energy, the general trends that it predicts are probably correct. As shown in Fig. 3a, the phase boundary for the four-component system can be represented as a curved surface in three-dimensional space. Compositions that correspond to points lying underneath this surface are unstable and will lead to phase separation between a dilute polymer solution and a dense complex phase. Fig. 3b shows the same phase diagram in two dimensions as a series of contour lines for different salt concentrations. Each contour line marks the border of the two-phase region for a given salt concentration. Several tie-lines are shown that connect the two co-existing phases. It should be noted that the salt concentrations in the two co-existing phases need not be equal, so that the tie-lines do not necessarily lie parallel to the P – Q plane in Fig. 3a. The Voorn–Overbeek theory predicts a slight accumulation of salt in the concentrated complex phase. Fig. 3c shows the binodal line for a stoichiometric mixture ($\phi_P = \phi_Q$) as a function of the salt concentration.

It can be seen in Fig. 3b that the two-phase region is centered around the line $\phi_P = \phi_Q$ that represents stoichiometric (1:1) charge compositions; tie-lines run somewhat parallel to it. Since a macroscopic phase cannot contain excess charge, off-stoichiometric compositions must take up charged species from the solution to achieve neutrality, either by means of proton transfer or by taking up counterions. In particular, the latter exert an osmotic pressure, which counteracts the cohesive forces in the complex. Therefore, the width of the two-phase region is a measure for the strength of these cohesive forces. For very asymmetric mixtures, the number of small ions that have to be taken up by the complex is very large and their entropy may inhibit macroscopic phase separation. Instead, smaller soluble complexes may be formed that carry an excess charge [51]. The Voorn–Overbeek theory does not account for such soluble complexes, so that the width of the two-phase region in Fig. 3b is probably overestimated.

When salt is added, the two-phase region shrinks progressively, and above a critical ionic strength, complexation is entirely suppressed. The critical salt concentration strongly depends on the type of ionic groups on the chain, on the charge density of the polymers, and on their length. In Table 1, we present our data for the critical salt concentrations for a number of polyelectrolyte pairs. These data show how widely the critical salt concentrations can vary from one pair to another.

Experimental phase diagrams have been measured for a number of systems [52–54]. In Fig. 4, we present our own recent experimental data [52] for strictly stoichiometric mixtures of PAA and PDMA-EMA in the presence of KCl. As can be seen, the two-phase region is strongly asymmetric, with very low concentrations for the dilute phase. The volume fraction of polymer in the complex phase

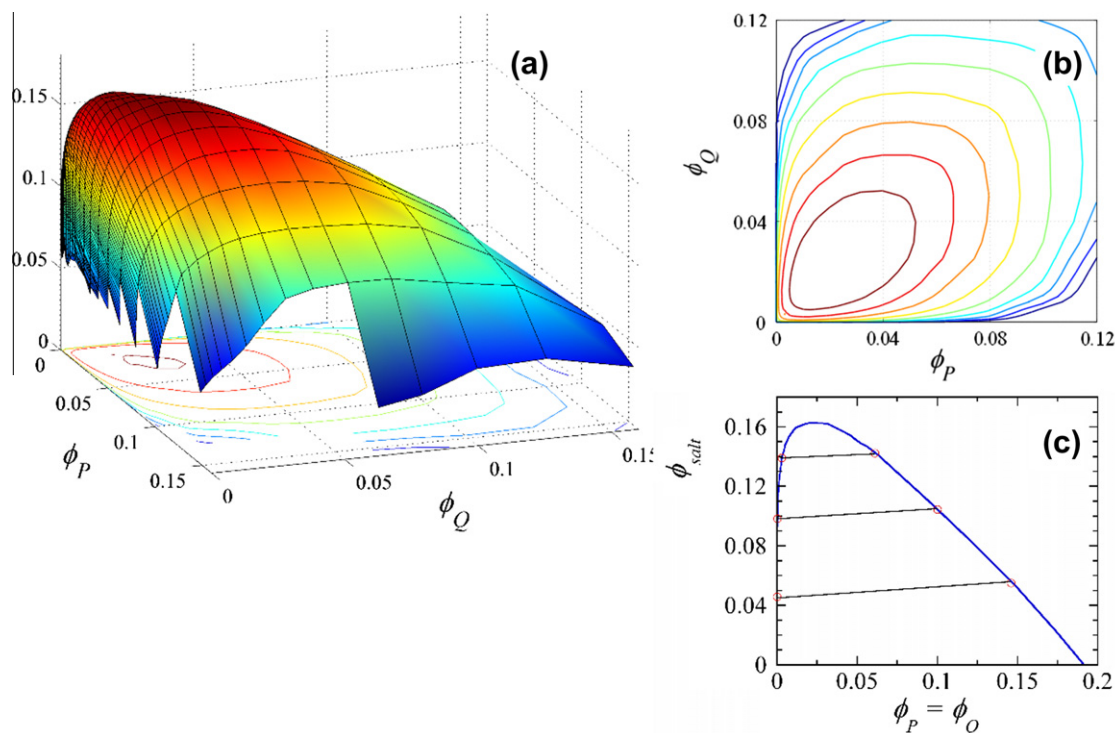


Fig. 3. Phase diagram for polyelectrolyte complexation calculated using the theory of Overbeek and Voorn [36]. (a) Three-dimensional representation of the phase diagram (ϕ_P : volume fraction of polycation, ϕ_Q : volume fraction of polyanion, ϕ_{salt} : volume fraction of salt; $N_P = N_Q = 100$). Compositions corresponding to points below the drawn surface are unstable. (b) Two-dimensional representation of the same phase diagram; binodal lines for different salt concentrations are shown, as well as three tie-lines connecting co-existing phases. (c) Binodal line and several tie-lines for a stoichiometric mixture of polyelectrolytes.

increases as the salt concentration decreases and reaches a limiting value of around 0.35. The lines in Fig. 4 are fits to the model of Voorn and Overbeek. It is clear that the width of the two-phase region depends on the length of the polymers; the critical salt concentration increases with increasing chain length. It was shown that the effect of chain length on the critical salt concentration could be explained by mapping the associative phase segregation onto the classical expression of Flory and Huggins for segregative demixing of polymer–solvent mixtures. For this, the Voorn–Overbeek expression for the free energy of a stoichiometric mixture was expanded in a power series of concentration. The prefactor of the quadratic term was then interpreted as an effective chi-parameter, which is a function of salt concentration rather than temperature [55]. This is a first indication that a stoichiometric mixture of polycations and polyanions can be considered in some respects as a common neutral polymer/solvent mixture. As we will show below, however, there are important differences.

2.5. Cohesive energy of a polyelectrolyte complex

In order to determine the strength of the cohesive ion–ion pair forces in a polyelectrolyte complex, we attached polyelectrolytes of either sign as brushes to a solid surface in a colloidal probe AFM configuration (Fig. 5a) [56]. One surface was a flat oxidized silicon wafer; and the other was a silica colloid of 3 μm radius glued to the cantilever spring. The surfaces were immersed in aqueous solutions with varying salt concentration. During a typical experimental approach-and-retract cycle (Fig. 5a), the brushes come into contact and form a thin complexed layer. Initially, the brushes on both sides of the complex layer are compressed, but as the brushes are kept in contact, they start to interpenetrate. This interpenetration is driven by the growth of the complex phase on both sides of the initial layer. When the surfaces are separated again, the polyelectrolyte chains are stretched until enough energy is stored to

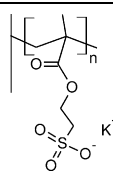
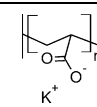
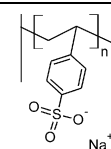
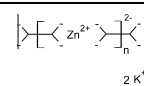
disrupt the complex phase. In this case, disruption involves breaking all formed ion–ion pairs between the brushes.

The force–distance curves corresponding to this cycle show that the ion–ion pair forces depend strongly on salt concentration. Fig. 5b–d presents a few examples for PTMAEMA and PSPMA brushes. At salt concentrations above 1.5 M, the interaction between the positive and the negative brushes is simply repulsive (Fig. 5d). At about 1.5 M, attraction sets in as can be seen in both approach and retraction curves. This salt concentration is the equivalent of a critical salt concentration for complex coacervate phases (see above). As long as the attraction remains weak, that is, in a narrow window close to the critical salt concentration (e.g. Fig. 5c for 1.4 M), an almost reversible approach–retraction cycle is possible, when scanning slowly and avoiding extensive compression of the brushes. Reversibility is the result of formation and breaking of ion–ion pairs in the initial contact layer without subsequent growth of the complex phase. Further away from the critical point, and for larger scan rates, the attraction increases dramatically and soon reaches the limits of the instruments' dynamic range (Fig. 5b). This is accompanied by a large approach/retraction hysteresis. At these large attractive forces, we observe erosion of the brushes: when cycling repeatedly, the attractive force is gradually and systematically weakened. Erosion occurs faster at lower salt concentrations and hence larger attractive forces. In line with the weakening of the attractive force, we found that the ellipsometric thicknesses of the brushes after drying decrease in the same gradual manner. Clearly, the forces exerted to separate positive and negative chains are strong enough to break covalent bonds, showing that the cohesive interactions that hold the complex together are very large, up to hundreds of kT per chain.

Another way to probe the cohesive interactions in a material is to measure its interfacial tension. For the biphasic polyelectrolyte system, this implies measuring the interfacial tension between the dilute and the concentrated phase. We have measured interfacial

Table 1

Critical salt concentrations in M for complexation between various polyelectrolytes. Values correspond to concentrations of KCl unless stated otherwise. All mixtures were prepared at a 1:1 stoichiometric ratio of polymeric charges and an overall concentration of polymeric charges of 0.050 M. All mixtures were prepared at pH 6.5, where all weak polyelectrolytes are strongly charged ($\sigma > 0.95$). For every combination, several mixtures at varying KCl concentration were prepared. The critical salt concentration was taken as the average between the highest salt concentration for which complexation was observed and the lowest salt concentration for which a homogeneous solution was obtained. Complexation was judged either by eye (macroscopic phase separation) or by optical microscopy (small flocs or droplets). The polymer specifications are as follows. PDMAEMA: polymer source, $M_n = 23.5$ kg/mol, $M_w/M_n = 1.04$; PTMAEMA, synthesized by ATRP, $M_n = 19.7$ kg/mol, $M_w/M_n = 1.3$; P2MVP, polymer source, $M_n = 18.0$ kg/mol, $M_w/M_n = 1.09$, degree of quaternization 70%; PEI, Sigma Aldrich, 50% (w/v) solution in water, molar mass unknown; PAH, Sigma Aldrich, $M_n = 6$ kg/mol, $M_w/M_n = 2.5$; PAA, polymer source, $M_n = 10.0$, $M_w/M_n = 1.15$; PSPMA, synthesized by ATRP, $M_n = 21.4$, $M_w/M_n = 1.3$; PSS, polymer source, $M_n = 34.0$, $M_w/M_n = 1.03$, degree of sulfonation 99%.

Polycation	Polyanion N	PSPMA 94	PAA 147	PSS 170	L_2EO_4/Zn^{2+} n
	N				
PTMAEMA	95	1.1 ± 0.05	0.65 ± 0.13	0.02 ± 0.01	–
PDMAEMA	151	1.2 ± 0.05	1.2 ± 0.05	0.04 ± 0.03	0.55 ± 0.13
P2MVP	88	1.4 ± 0.04	0.60 ± 0.08	1.9 ± 0.12	0.41 ± 0.12
PAH	80	3.2 ± 0.5	>10 (NaNO ₃), >6.5 (NaCl), >3.5 (KCl)	1.8 ± 0.3	1.0 ± 0.13
PEI	?	1.9 ± 0.3	>10 (NaNO ₃), >6.5 (NaCl), >3.5 (KCl)	0.70 ± 0.08	–

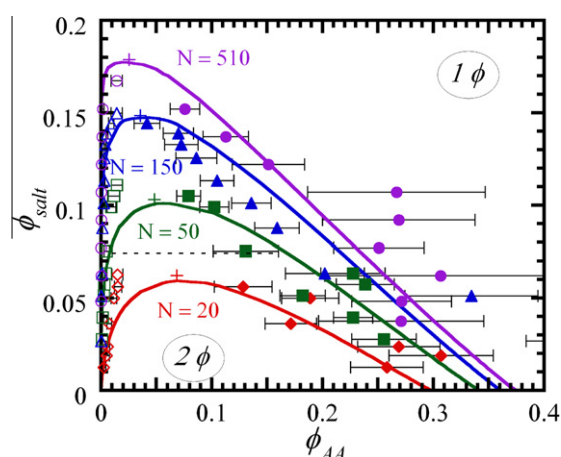


Fig. 4. Experimental phase diagram for stoichiometric mixtures of PAA and PDMAEMA of various chain lengths with added KCl [52]. Lines are fits to the Voorn–Overbeek theory.

tensions for the same set of polyelectrolytes as described above (i.e., PTMAEMA and PSPMA) at varying salt concentrations [57] using the method proposed by Sprakel et al. [58] This method allows determining the interfacial tension of liquid–liquid phases at binodal composition. To achieve this, the strength of a capillary

bridge of one of the two phases is measured in a colloidal probe AFM configuration as a function of separation between flat surface and colloidal probe (Fig. 6a). In order to calculate the interfacial tension, one needs only the dimensions of the colloidal probe and the contact angle at the interface of the two liquids at the surface. We determined the contact angle of a complex coacervate phase in equilibrium with its dilute phase for all salt concentrations (Fig. 6b). The interfacial tensions so measured are presented as a function of the salt concentration in Fig. 6c [57].

The interfacial tensions decrease with increasing salt concentration and vanish at a critical salt concentration $c_{cr} \approx 1.3$ M, similar to that seen for the interaction between two oppositely charged brushes discussed above. It was found that the interfacial tension decreases as $\gamma \sim (c_{cr} - c_{salt})^{3/2}$ over a wide range of salt concentrations (see inset Fig. 6c). This scaling could be explained by treating the polyelectrolyte complex as an effective neutral polymer with a salt-dependent polymer–solvent interaction parameter [57]. Quantitatively, the interfacial tensions are surprisingly low, namely in the order of 100 μ N/m. We can obtain a measure for the typical length scale in the complex phase using $\gamma \approx kT/\xi^2$, giving $\xi \approx 3$ –10 nm, which is roughly the size of an individual chain. Such a low interfacial free energy of only a few kT per polymer chain is rather unexpected, given the strength of the electrostatic interaction that manifests itself in the ion pairs separation experiment shown in Fig. 5. It implies that the creation of extra surface area does not require the rupture of ion pairs, but only their redistribution.

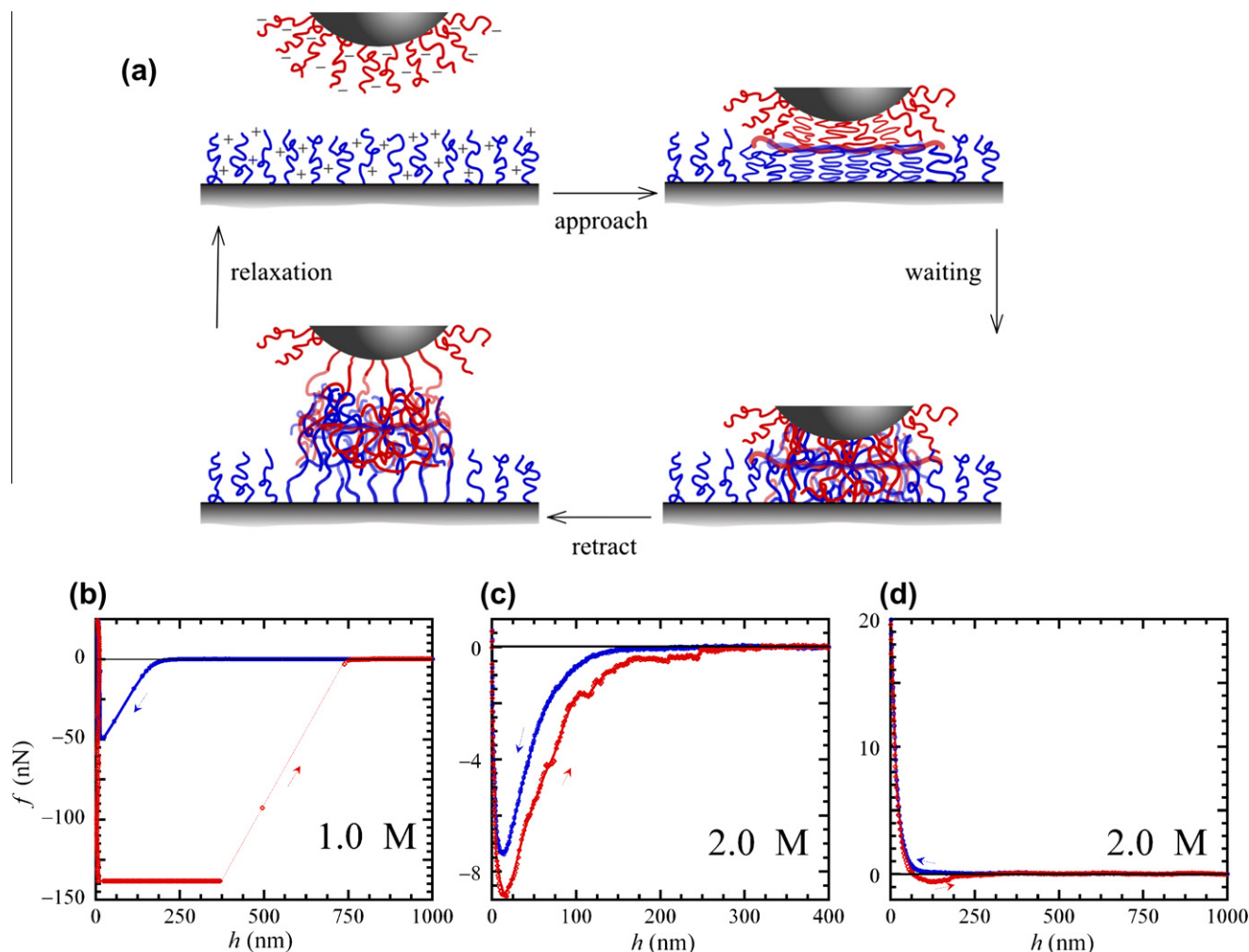


Fig. 5. (a) Schematic picture showing the AFM measurement of the interactions between two oppositely charged polyelectrolyte brushes. (b–d) Measured force–distance curves between a surface covered with a PTMAEMA brush and a surface covered with a PSPMA brush for KCl concentrations of 1.0 M (b), 1.4 M (c), and 2.0 M (d) [56].

Apparently, the cohesive energy between different ion pairs is only small.

These two different sets of AFM experiments demonstrate that the work that has to be done to break up a polyelectrolyte complex depends strongly on how it is broken up. If the oppositely charged polyelectrolytes are separated from each other, as in the case of the oppositely charged brushes (Fig. 5), all the ion pairs must be broken, requiring energies that can amount to hundreds of kT per polymer chain. By contrast, if a polyelectrolyte complex is split into two smaller, but still neutral complexes, no ion pairs must be broken and the required work, associated with creating extra interface, is only a few kT per chain. This distinction can have important consequences for the dynamics and mechanical properties of microphases based on assembly of these polyelectrolytes: for small complexes that consist of only a few chains, it may become impossible to split the complex without separating positive from negative charges. This will show up as an extra penalty.

2.6. Dynamics in polyelectrolyte complexes

Because we find the cohesive energies between different ion pairs in a polyelectrolyte complex to be rather small, we should expect that the polymers in a complex can still move with respect to each other. Indeed, many polyelectrolyte complexes behave liquid-like (in this case, they are called complex coacervates), although some polyelectrolyte pairs form solid precipitates at low salt

concentration [54]. The dynamics of polyelectrolyte complexes can be probed using rheological measurements [59]. Recently, we have shown that both PTMAEMA/PSPMA and PDMAEMA/PAA complex coacervates are viscoelastic [60]. With increasing salt concentration, the relaxation times became shorter and the complexes behaved more liquid-like.

In Fig. 7a, we give the storage and loss moduli as a function of frequency, measured for the 1:1 complex coacervate of PAA and PDMAEMA (degree of polymerization of both is 500) for a range of salt concentrations [60]. These curves have the familiar shape of a viscoelastic fluid such as a polymer melt or a concentrated polymer solution, with the storage and loss moduli crossing at some typical frequency. At high salt concentrations, the complex coacervates behave liquid-like in our experimental frequency window, as deformations relax faster than they are typically applied ($<ms$). At low salt concentrations, they behave like soft solids, with storage moduli that are larger than the corresponding loss moduli and relaxation of deformations occurring slower than they are typically applied ($>1 s$). The interesting point is that the salt concentration influences the absolute values of the moduli, but not the shapes of the curves, so that we can simply make them coincide by shifting along the frequency axis and applying a minor correction to the modulus axis. A very similar behavior is found for polymer melts as a function of temperature, and the procedure of shifting the data to make them coincide is classically known as ‘time–temperature superposition’. Hence, the complex coacervates

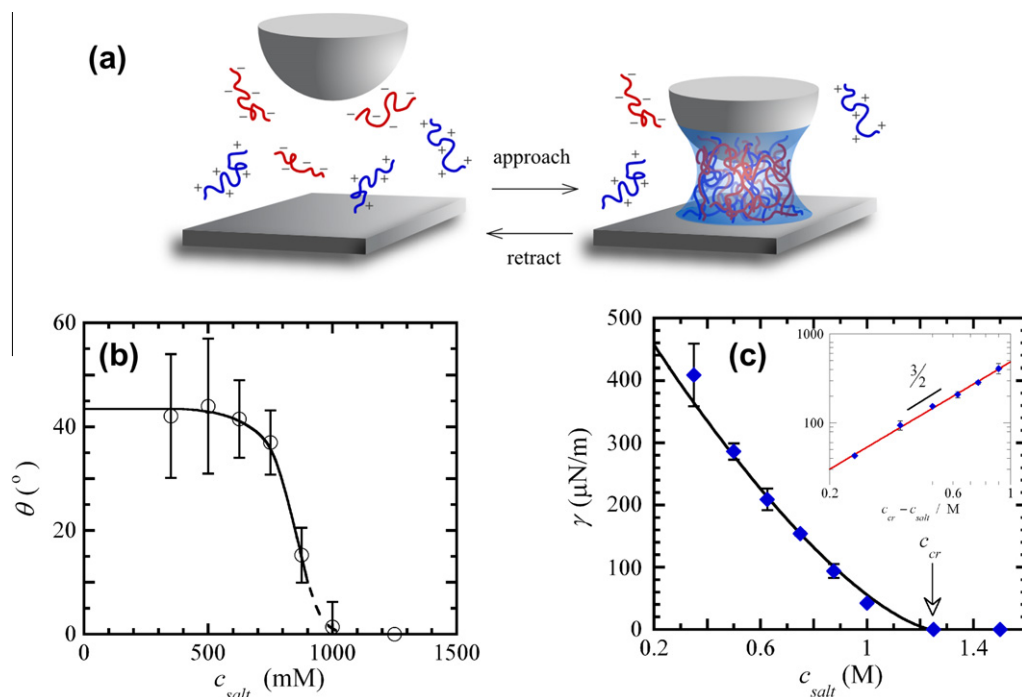


Fig. 6. (a) Schematic picture showing the AFM measurement of the interfacial tension of a polyelectrolyte complex phase. (b) Contact angle of a polyelectrolyte complex phase (PTMAEMA/PSPMA) in its coexisting dilute phase on silica as a function of KCl concentration. (c) Measured interfacial tension as a function of KCl concentration. Inset: interfacial tension as a function of $c_{\text{cr}} - c_{\text{salt}}$ on a double-logarithmic scale [57].

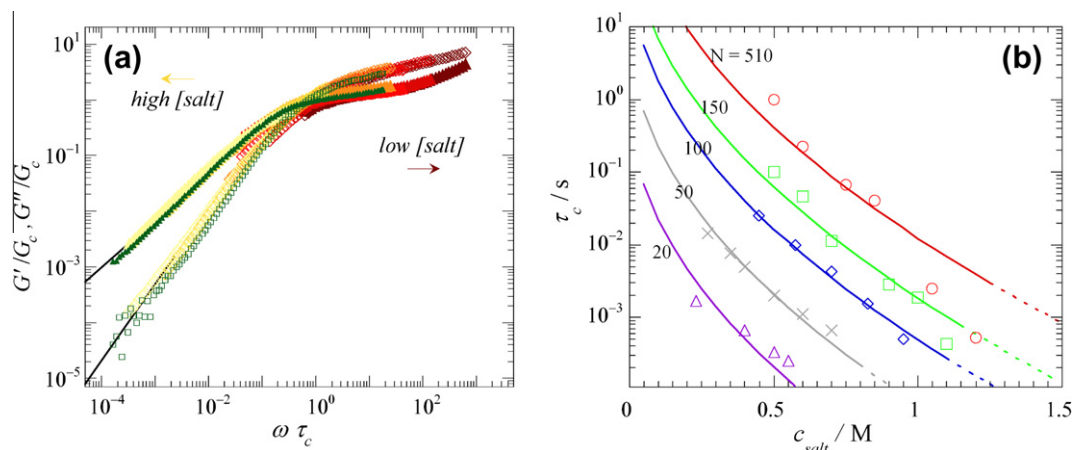


Fig. 7. (a) Dynamic modulus of a PDMAEMA/PAA complex (both with degree of polymerization of 500) for different KCl concentrations. The curves measured at different salt concentrations are super-imposed by using salt-dependent shift factors for the loss and storage modulus (G_c) and for the frequency (τ_c). (b) Time shift factors as a function of salt concentration for different chain lengths [60].

possess the property of ‘time–salt superposition’ (Fig. 7a). By choosing the shift factors such that the crossing point occurs at a rescaled frequency ($\omega \tau_c$) of 1, we can estimate the apparent relaxation time of these complex coacervates (τ_c). Fig. 7b shows the apparent relaxation time as a function of salt concentration and polymer chain length.

As the salt concentration decreases, we find that relaxation times increase slightly more than exponentially. The two longest polyelectrolyte chains seem to show an even stronger increase in relaxation time at their lowest salt concentrations. If we apply the analogy with common one-component polymer systems at varying temperatures here as well, we may expect a strong increase in relaxation times at sufficiently low salt concentrations. Just like the relaxation times of common polymers diverges at low temperatures, because they undergo a glass transition, the relaxation times of these systems may diverge at sufficiently low salt concentration, and the complex

coacervate phases could undergo a glass transition as well. This is indeed in line with the general observation that polyelectrolyte complex phases occur in true solid-like, i.e., mobile or quenched, states at low salt concentrations and in viscoelastic or liquid-like, i.e., mobile or annealed, states at higher salt concentrations [60]. The transition between the two should be regarded as a glass transition, as was suggested by Kovacevic et al. [61] and later by Weinbreck et al. [15]; unfortunately, data on such transitions are scarce.

3. Microphases of polyelectrolyte complexes

3.1. Polyelectrolyte multilayers

In 1992, Decher reported that he could make films of controlled thickness by exposing a surface to solutions of a polyanion and a

polycation in a cyclic fashion [62]. This became known as the ‘layer-by-layer’ (LBL) method and generated a lot of research activity to fabricate many kinds of films: on solid substrates [63–71], as free standing films (after removing the substrate) [72,73], or as hollow capsules (after dissolving the solid sphere serving as template) [74–77]. Varying the components, one can make a plethora of hybrid materials.

Clearly, these films are a particular representation of polyelectrolyte complex phases, and so one would expect there to be a general relationship between the phase behavior of polyelectrolyte complexes on the one hand and the LBL fabrication process on the other. Such a viewpoint was elaborated by Kovacevic et al. [61]. In order to explain the reasoning in that paper, let us refer to the complex coacervation phase diagram, in particular the cross-section in the plane defined by the polycation and polyanion concentrations (see Fig. 8a).

The cyclic exposure of a growing layer of insoluble complex phase to polyanion and polycation solutions can be represented in this diagram by a path connecting the horizontal and the vertical axes: upon replacing one solution by the other, the composition of the entire system somehow has to switch from polycation dominated to polyanion dominated. This involves crossing the binodal twice: once at the ‘cationic’ side and once at the ‘anionic’ side. As long as the overall composition is within the binodal, the system is biphasic, meaning that the (dense) film of complex is also stable. However, if a thin film of coacervate, containing only a small amount of complex, is exposed to a substantial volume of a one-component polyelectrolyte solution, the overall composition must be well outside the two-phase region. This implies that the deposited layer (provided it can equilibrate) should *redissolve* in the form of charged soluble complexes, as illustrated by the cartoon in Fig. 8b.

What Kovacevic et al. found was that such dissolution indeed takes place. First, immediately after the solution switch, an

increase in thickness and film mass is found; this can be seen as the consequence of entering the two-phase region, leading to additional formation of the concentrated phase. In molecular terms, it means that the layer picks up polyelectrolyte of opposite charge, thereby neutralizing and even over-compensating its surface charge to a certain degree. What happens next depends on the ionic strength. At low salt concentration (Fig. 8c), the increase quickly levels off to a stable value, meaning that no more polyelectrolyte can bind nor leave the surface. At higher salt concentration, however, a slow but very clear *decrease* of the film’s mass occurs, which seems to continue for a long time (Fig. 8d). Clearly, the layer is not stable under these conditions, as expected from the phase diagram, and the corresponding molecular picture is that polymers are pulled off the surface by their oppositely charged counterparts, forming soluble complexes (Fig. 8b). Since full equilibrium implies that the complex phase should not exist outside the binodal region, the layer should eventually dissolve entirely. However, the rate at which this occurs is slow. Moreover, this rate drops dramatically when the salt concentration is decreased, from which the authors tentatively infer that below a certain threshold salt concentration all translational mobility in these complex phases is lost altogether, like in a glass (Fig. 8e). The authors call that threshold a ‘glass transition salt concentration’.

The study of Kovacevic et al. made clear that polyelectrolyte complexes can switch from equilibrating (at high salt) to essentially frozen (at low salt). As discussed above, rheological studies point in the same direction. In the high-salt case, the LBL film exposed to excess polyelectrolyte is clearly unstable, but in the low-salt case, it must be regarded as metastable. This can have unusual behavior as a consequence. For example, hollow spherical capsules fabricated by the LBL method were reported to unexpectedly *increase* in size upon changing the pH when the complex was sufficiently plasticized by adding salt [78,79]. The polyelectrolyte

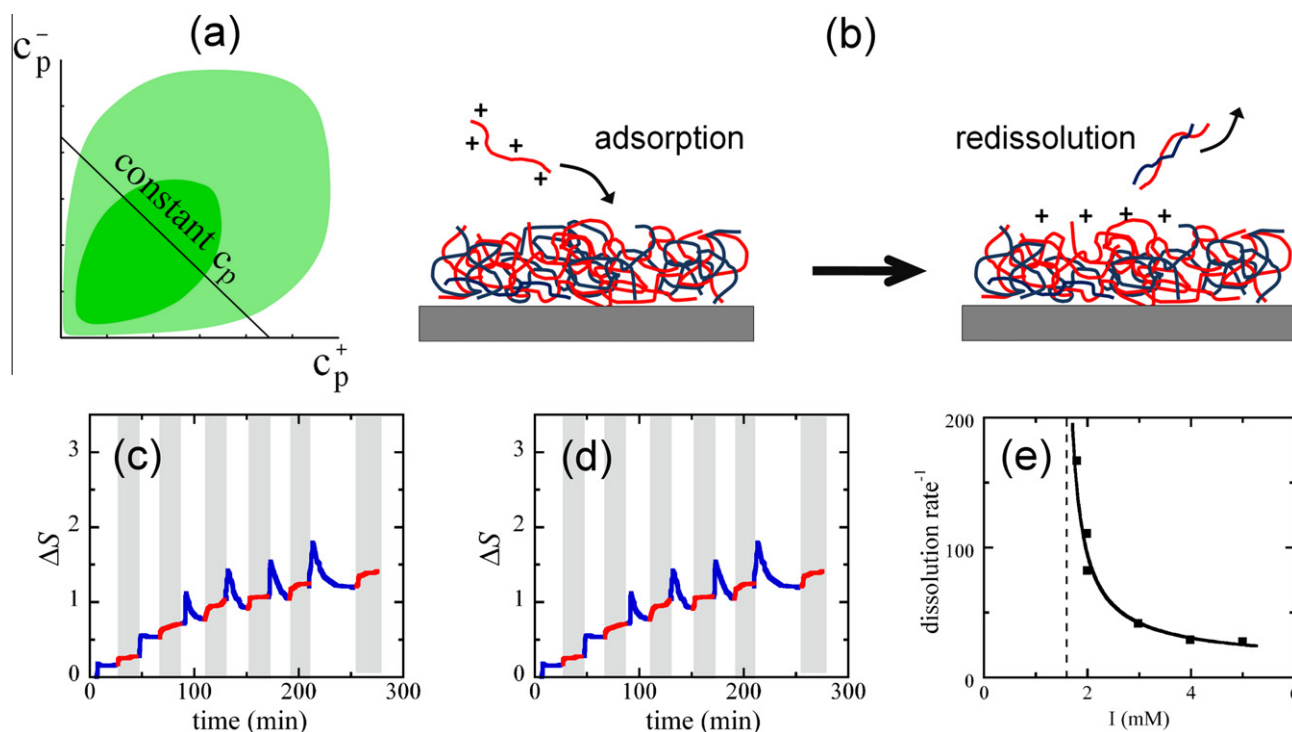


Fig. 8. (a) Phase diagram of polyelectrolyte complexation for two salt concentrations (light green: low salt; dark green: high salt). The line of constant polymer concentration represents the cycling between excess polyanion and excess polycation. (b) Schematic picture showing the redissolution of a coacervate film when it is exposed to excess polycations, outside the two-phase region. (c and d) Multilayer formation on silica by sequential addition of PDMAEMA and PAA at 1 mM (c) and 5 mM (d) salt. The measured reflectometer signal ΔS is proportional to the adsorbed amount of polyelectrolyte. Blue lines on white background denote addition of PDMAEMA; red lines on gray background denote addition of PAA. (e) Dissolution rate of the coacervate film as a function of salt concentration. The vertical dashed line indicates a glass transition (c and d adapted from Kovacevic et al. [61]).

pair here was PAH/PMA, both of which are weak polyelectrolytes with a pH-dependent charge. At low pH, protonation of the PMA chains leaves the whole complex with a net positive charge. The observation that this leads to an increase in film area points to a change of sign of the interfacial tension from positive to negative. Obviously, this cannot be a stable state. This supports the point of view that one can have states which cannot be thermodynamically stable, yet persist, so that they must be metastable.

There is yet another way in which growing polyelectrolyte complex films respond to the cyclic nature of the LBL method when the layer is not entirely frozen. This case is called 'exponential growth', and it is characterized by the fact that the amount of additional polymer complex (dm) deposited per cycle (dn) increases roughly linearly with the film mass m when the layer gets thicker. This implies that m itself increases exponentially with n . The explanation proposed by Schaaf et al. [80,81] requires that (1) one component in the film is mobile and (2) the composition adopted by the complex shuttles during the LBL cycle between two values: one somewhat enriched in positive polymer and the other enriched in the negative. Indeed, inspection of the generic phase diagram (Fig. 8a) shows that these two compositions correspond to the two binodal points at the cationic and anionic side, respectively. The difference between these two values corresponds to an excess amount of mobile (say, positive) component throughout the complex film, which is available for complexation when the other (negative) component is supplied from the solution side. The consequence is that during exposition to a solution of the negative polyelectrolyte, an amount of complex is deposited, which has recruited all this positive mobile excess contributed by the *entire* layer [80–82]. In the second part of the cycle, the excess mobile component is restored by exposure to the solution of this mobile component. It is not entirely clear why dissolution does not occur in this case; perhaps, the rather extreme mismatch between chain lengths (one very short, one very long) plays a role.

The existence of frozen and mobile states has also consequences for the internal structure of the film. Frozen films will reflect the history of the sample's preparation and therefore be stratified in alternating zones of polycation and polyanion, as was demonstrated by Decher for PSS/PAH [63]. In partially mobile films (with one mobile component), sample history is also conserved, although anion/cation stratification does not occur. For example, when the immobile component is labeled during one particular cycle, this shows up as a labeled zone in the film [82,83]. In fully mobile films, however, any stratification is irretrievably lost due to polymer mobility: such films must be considered as amorphous fluid complexes (complex coacervates) and as instances of wetting films. This justifies the question whether or not such films are in the complete wetting regime, with a laterally homogeneous thickness, or in some partial wetting regime, which causes them to break up into droplets. For the example of PTMAEMA/PSPMA on silica, we saw that partial wetting occurs for KCl concentrations up to 1 M (see Fig. 6b).

3.2. Zipper brushes

Although polymer brushes can in principle be made through adsorption of an appropriate diblock copolymer, attempts to do so are not very successful. The problem is that the required surface selectivity (one block for anchoring, the other to dangle in solution) is difficult to achieve in practice. Having one insoluble block promotes stronger adhesion to the substrate, but also tends to induce micellization in solution, which is unfavorable for adsorption. Selective adsorption is very difficult to implement in chemical terms. Hence, brushes prepared by adsorption from solution tend to have low densities or a poorly defined lateral structure [84].

There is one exception, which is based on polyelectrolyte complexation, namely the so-called zipper brush [85,86]. This brush is prepared by first making a thin layer of polyelectrolyte (either as a brush or as a thin film of gel) firmly anchored to the substrate. Any form of grafting-from or grafting-to can be employed. The making of the final brush follows in the next step, by adsorption from solution of a diblock copolymer with an oppositely charged block (Fig. 9a). The surface grafted and the free polyelectrolyte blocks form a complex, which collapses to a dense and thin layer, from which the neutral block protrudes as a brush. Since the composition of the complex (which is close to charge-stoichiometric) controls the number of chains taken up by the surface, the brush density σ is also to a large extent controlled by charge stoichiometry, i.e., the product of the number of charges in the polyelectrolyte N and the surface density of chains σ should be the same for the grafted (attached) and the adsorbed (free) polyelectrolyte chains: $N_{att}\sigma_{att} = N_{free}\sigma_{free}$. Since $\sigma_{brush} = \sigma_{free}$, this implies that a kind of 'leverage rule' applies: the number per unit area of neutral chains forming the brush is equal to that of the attached chains times a 'leverage factor' N_{att}/N_{free} . Hence, short charged blocks on the adsorbing (free) polymer and long chains grafted to the surface will lead to an enhanced density. Indeed, enhancement factors of order 10 and surface densities of the order of 1 nm^{-2} have been realized with this method, without compromising the control over chain length that one has with pre-synthesized polymers. Moreover, the preparation and modification of the zipper brush is very easy, as the adsorbed chain can be simply removed (unzipped) by means of concentrated salt or an acidic solution (Fig. 9b). This may be a very effective anti-fouling concept.

3.3. Charge-stabilized colloids and soluble complexes

While polyelectrolyte complexation at stoichiometric charge conditions usually leads to macroscopic phase separation, smaller complexes can be prepared at non-stoichiometric mixing ratios. Kabanov and Zezin [87] and Tsuchida [88] showed that careful mixing of two oppositely charged weak polyelectrolytes with significantly different molar mass leads to the formation of water-soluble complexes. These complexes consist of one molecule of the high molar mass polymer, decorated with a few shorter chains of opposite charge. When a small amount of salt is added to these soluble complexes, they can rearrange, which leads to aggregation into larger insoluble complexes. At very high salt concentration, the complexes dissociate completely [2,3,87].

Pairs of strong polyelectrolytes with comparable molar mass usually form highly aggregated, insoluble complexes. However, at very high dilution and at non-stoichiometric mixing ratios, it is possible to form colloidal particles with sizes in the range of a few hundred nanometers [2,3,34,35]. These particles are not in a state of thermodynamic equilibrium, but they are kinetically stabilized by an excess charge, which prevents further aggregation. Upon addition of salt, the particles first flocculate, before they dissociate at very high salt concentration [34,35]. The size, polydispersity, and shape of the complex particles depend on the preparation method, on the salt concentration, and on the nature of the polyelectrolyte chains. For example, needle-like particles were observed for complexation between poly (maleic acid-co-propylene) (PMA-P) and poly-L-lysine (PLL) [89]. The PLL chains in this complex adopt a stiff α -helical configuration, which causes the particles to become elongated.

3.4. Complex coacervate core micelles

Harada and Kataoka [90] and Kabanov et al. [91] were the first to realize that the availability of charged/neutral diblock copolymers opened a way to make nanoparticles by polyelectrolyte complex formation. The idea is that the charged block, when brought

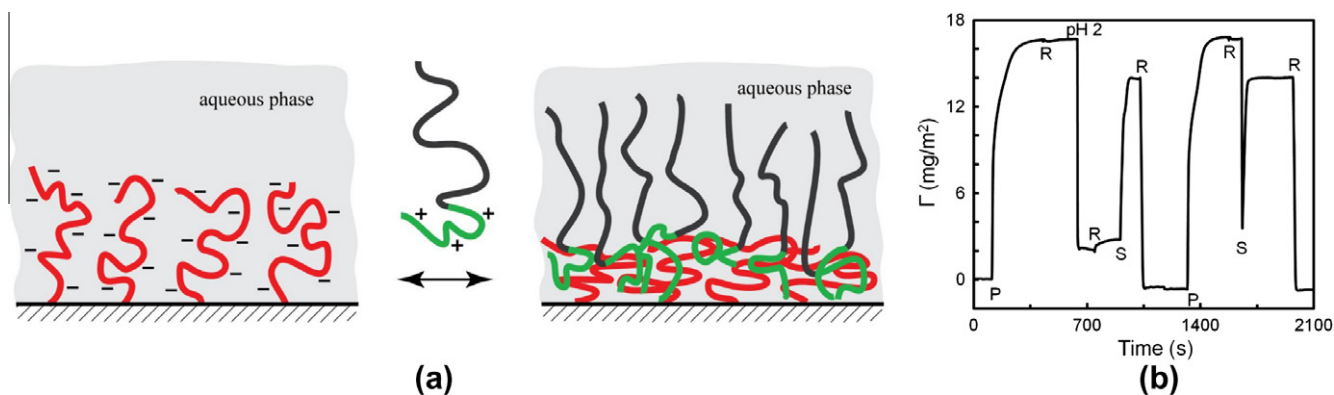


Fig. 9. (a) Schematic picture of the formation of a zipper brush by adsorbing a P2MVP–PEO diblock copolymer onto an oppositely charged grafted PAA layer. (b) Adsorbed amount as measured with optical reflectometry. P: addition of diblock copolymer; R: rising with solvent (pH 6); pH 2: rinsing with 0.01 M HNO₃; S: rinsing with a non-ionic surfactant solution [86].

together with an oppositely charged polymer, forms an insoluble complex surrounded by neutral, soluble chains (Fig. 10a). In other words, a tiny amount of insoluble phase appears that does not grow any further due to the presence of the neutral chains. This situation is very similar to that of insoluble apolar chains, which form a nanoparticle in water whenever they have one end carrying a polar, water-soluble moiety. Since we commonly use the term ‘micelles’ for these latter nanoparticles, it is quite logical to denote the polymeric nanoparticles based on polyelectrolyte complexation also as ‘micelles’. We have adopted the term ‘complex coacervate core micelles’ (C3Ms) [92]; others have used the terms ‘polyion complex micelles’ (PIC) [90], ‘block ionomer complexes’ (BIC) [91], or ‘inter-polyelectrolyte complexes’ (PEC) [93,94]. For an extensive recent review, see Voets et al. [95].

That there is a clear correlation between the formation of a C3M and the phase diagram of the corresponding polyelectrolyte pair is seen when the composition is varied and the formation of nanoparticles is followed, e.g., by means of light scattering [96]. A typical example is presented in Fig. 10b.

In this diagram, the composition (horizontal axis) is expressed in terms of the mole fraction f^+ of positive polymeric charges, with $f^+ = n^+/(n^+ + n^-)$, where n^+ and n^- denote the total number of positively and negatively charged groups on the polyelectrolyte chains. Hence, the composition runs from pure negative ($f^+ = 0$) to pure

positive ($f^+ = 1$) polyelectrolyte, and a stoichiometric mixture corresponds to $f^+ = 0.5$. As can be seen, the intensity is low for the pure polyelectrolyte solutions and increases towards stoichiometry. Initially, the increase is usually weak, indicating the formation of particles just somewhat larger than individual molecules (e.g., dimers and trimers) most likely carrying excess charge. These objects would be analogous to the ‘soluble complexes’ postulated by Kabanov and Zezin [87]. Upon further approaching stoichiometry, either from the negative or from the positive side, there is a sudden change in slope of the curve at about $f^+ = 0.4$ (negative side) or 0.6 (positive side), signaling the appearance of micelles. In this middle range, which is equivalent to the two-phase region in the phase diagram (see Fig. 3), the scattered intensity increases steeply to reach a maximum at about $f^+ = 0.5$, the stoichiometric composition. The size of the particles that dominates the scattering in this range is roughly constant, typically between 20 and 25 nm radius, suggesting that we are dealing with particles of a fixed size, but growing in number. This implies that the soluble complexes are gradually converted into micelles by uptake of the minority species, so that the concentration of ‘free’ (uncomplexed) charged groups almost vanishes at the peak position ($f^+ = 0.5$). Support of this conclusion comes from monitoring the pH around the peak (Fig. 10c). If we employ polyelectrolytes with weakly (de)protonating groups such as carboxyls and amines, micellization will generally involve an uptake or a release of protons,

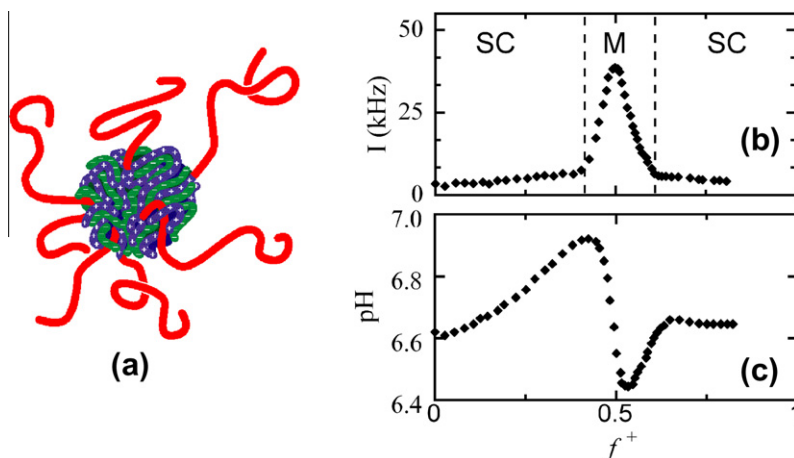


Fig. 10. (a) Schematic picture of a complex coacervate core micelle formed by association of a charged–neutral diblock copolymer and an oppositely charged polyelectrolyte. The insoluble complex coacervate core is stabilized by the soluble blocks that form the corona. (b) Light scattering intensity as a function of composition for a titration of PAA–PAAm with PDMAEMA. Micelles (M) are formed around the stoichiometric charge composition. Soluble complexes (SC) are formed at compositions away from stoichiometry. (c) pH as a function of composition for the same experiment.

depending on the pH. This would lead to a change in pH, but any uncomplexed polyelectrolyte will act as a buffer so that the rate of change is small as long as there is enough buffering capacity, i.e., as long as there is enough uncomplexed polyelectrolyte. This implies therefore that pH changes will be largest when the concentration of soluble complexes is lowest. In other words, $|dpH/df^*|$ has a maximum when the scattering has a maximum [96]. This is indeed what the pH curve in Fig. 10c shows.

A striking finding was reported by Harada and Kataoka for micelles with polylysine and polyglutamate as the polycation/polyanion pair. These would *selectively* take up a particular polylysine chain length from a mixture of chains of different lengths (but given polyglutamate length) [97]. A possible explanation for this could be that the width of the two-phase region for a mixture of polyelectrolytes of precisely matched length is much wider than that for an unmatched pair. The reason is that unmatched pairs will form complexes with excess charge (which are soluble), whereas the matched pair cannot do so. Hence, when an excess of polylysine, containing several chain lengths, is added to a solution of (monodisperse) polyglutamate, micelles can form from length-matched pairs, but not from unmatched pairs (because these remain soluble), so that the uptake of the matching chain length is selective. The same argument would hold for any mixture of a monodisperse polyelectrolyte with an excess of oppositely charged chains containing several chain lengths.

3.4.1. Critical micelle concentration and aggregation number of C3Ms

Micelle formation generally occurs when the concentration of aggregating monomers exceeds a critical value, the so-called critical micelle concentration (CMC). The value of the CMC is directly related to the free energy of micellization, which is determined by a balance between the attractive interactions holding the chains in the core together on the one hand and the repulsive interactions between corona chains and chain deformation entropies on the other [98]. For C3Ms, the CMC depends on the salt concentration [99–101]. Addition of salt weakens the electrostatic driving force for complexation (see Fig. 2) and therefore causes an increase in the CMC. As discussed above, a stoichiometric mixture of polycations and polyanions can be treated in some respects as a common neutral polymer/solvent mixture with a polymer–solvent interaction parameter that depends on the salt concentration [55,57]. Using this, Wang et al. [100] showed that the CMC of C3Ms should increase with salt concentration as $CMC \sim \exp(a \cdot c_{salt}^{1/2})$, with a constant a that depends on the charge density on the chains. This was found to be in very good agreement with experimental data. Salt also has an effect on the mass of the micelles. With increasing salt concentration, the aggregation number of the C3Ms decreases in an almost linear fashion [100]. This observation could be explained using the above-mentioned salt dependence of the interfacial tension of the polyelectrolyte coacervate phase.

Another important parameter that affects the micellar size is the ratio between the lengths of the charged block and the neutral block of the diblock copolymer. When this ratio is small, we have ‘starlike’ micelles with a low aggregation number, a small core and a thick corona; when it is large, one gets ‘crewcut’ micelles with a high aggregation number and a thin corona. The ‘overall’ size, well represented by the hydrodynamic (diffusion) radius, is of course the sum of the core and corona sizes and, hence, much less sensitive to the length ratio. Voets et al. [102] investigated micelles based on three PAA–PAAm diblocks with P2MVP as the positive homopolymer by means of small-angle neutron scattering (SANS) and light scattering. From the shortest to the longest neutral block, aggregation numbers (=number of diblock copolymers per micelle) fell from 45 to 15, whereas the hydrodynamic radii increased from 16 to 20 nm. The radii obtained from static scattering increased likewise. Of course, when the corona block becomes too short, micelles

become unstable and prone to aggregation. Aggregation numbers also become smaller when one takes two diblock copolymers instead of one diblock plus one homopolymer [28]. This doubles the number of chains and leads to more crowding in the corona, which favors smaller micelles, because these have a large surface area-to-core volume ratio.

The core of the micelles discussed so far have a fixed area-to-volume ratio, as their volume is fixed by the number of monomer units in the charged block of the block copolymer employed. However, as shown by Hofs et al. [103], it is possible to swell the core by adding extra insoluble core material, in the form of complex coacervate, to the mixture. This is analogous to adding oil to a system of conventional surfactant micelles. Since (equilibrated) systems of oil-swollen micelles are commonly referred to as ‘micro-emulsions’, we tend to call coacervate-swollen C3Ms (when equilibrated) ‘complex coacervate core micro-emulsions’. For such objects, the size should follow a simple law based on specific surface area, since the amount of area is fixed by the amount of corona chains, whereas the volume is varied proportionally to the amount of homopolymer. Not all systems studied by Hofs followed this law, showing that equilibration does not easily occur, but at least this simple method allows the fabrication of colloidal particles consisting of polyelectrolyte complex in a wide range of sizes.

3.4.2. C3Ms with a demixed corona

A unique feature of these charge-induced polymer micelles is that they can bring polymeric components together in one particle that would normally not mix spontaneously. For example, two chemically different, uncharged polymers in a common solvent will often phase separate. By connecting each of these polymers to a differently charged block, it should be possible to bring two such polymers together in the corona of a C3M. We wondered whether some form of segregation would take place under these conditions. The simplest (average) structure a micelle could have in this case is a dipolar arrangement with the different polymers arranged around the two poles (Fig. 11a). Self-consistent field calculations [104] show that demixing of mobile chains attached to the surface of a micelle with a spherical core does indeed occur, provided that the two polymers are sufficiently incompatible. Voets et al. [105] studied mixtures of PAA–PAAm and P2MVP–PEO and found that micelle-like nanoparticles were indeed found, but assessing the detailed morphology of such particles at the nanoscale proved to be a major challenge. An important piece of evidence was found in NMR-NOESY experiments, which unambiguously showed that the PAAm and PEO blocks did not have close contacts between each other, thereby strongly supporting the picture of a demixed corona. Small-angle neutron scattering (SANS) and X-ray scattering (SAXS) data, together with cryo-TEM micrographs, demonstrated that the assemblies had a disk-like core about 16–20 nm in diameter, whereas depolarized light scattering data provided evidence that the particles were prolate ellipsoids with a long axis of about 45 nm. Altogether, this is consistent with a morphology as sketched in Fig. 11a: a central disk-like core consisting of polyelectrolyte complex from which two ‘lobes’ protrude, one formed by PAAm blocks and one formed by PEO blocks [106].

A related property of a demixed-corona micelle is its ability to form finite-size aggregates when one of the corona species is in a poor solvent, while the other remains well solvated. For example, micelles with a corona consisting of PEO and PNIPAM will have a tendency to aggregate at temperatures above the LCST of PNIPAM, but the presence of PEO, which has a much higher LCST, will prevent indefinite growth of such aggregates. As a result, a new supramicelle is formed with a well-defined size, see Fig. 11b. An example of this was reported by Voets et al. [107]; upon changing the temperature between 20 °C and 60 °C, these micelles underwent a reversible, 16-fold change in mass per micelle.

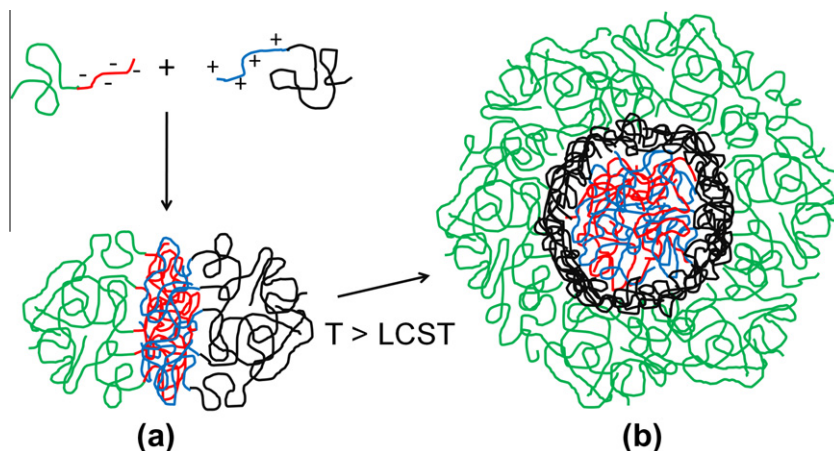


Fig. 11. (a) Schematic picture of a 'Janus micelle' with a demixed corona, formed by mixing two diblock copolymers with oppositely charged polyelectrolyte blocks and different neutral blocks. (b) A supramicelle formed by temperature-induced association of Janus micelles.

3.4.3. Filled C3Ms

A rather special variant of C3Ms is a mixture of a charged/neutral block copolymer with a *reversible supramolecular polyelectrolyte* (RSP). An RSP is a (charged) water-soluble chain formed from smaller subunits, which can each bind reversibly to exactly two neighbors; our example here is a coordination compound formed from a bisligand and appropriate metal ions (see Fig. 12a and b) [108].

A typical feature of these RSPs is that they can often both form rings and linear chains. At low concentration, rings or short chains are the dominating species, but at high concentration chains take over, increasing in length as the concentration goes up [108]. Yan et al. [5109] found that C3Ms were formed when homopolyelectrolyte was replaced by this coordination compound, even at concentrations where the dominating species in solution was a cyclic dimer carrying four charges (Fig. 12c). Molecules with the same number of charges, but unable to form chains, did not lead to micellization. The explanation is that the coordination compound accumulates near the oppositely charged (cationic) block and then polymerizes, thereby driving the phase separation that underlies micellization. A light scattering study as a function of mixing ratio shows that on the negative side, where there is an excess of coordination compound, there is more scattering than for systems with conventional (covalent) polyelectrolyte, showing that the two-phase region in the phase diagram extends to higher f^- in this case (Fig. 13a). This probably means that soluble complexes with a 'dangling end' of excess coordination compound are not stable. This is indeed expected at low concentration where the coordination compound does not polymerize. The micelles formed in this system show up nicely in cryo-TEM micrographs because of the metal in the core, which provides high contrast (Fig. 13b).

Instead of homopolymers or coordination polymers, one can use proteins to make C3Ms, because these can also carry charges (although much less than typical polyelectrolytes) [110]. This was exploited by Lindhoud et al. to obtain micelles with enzymes in their core [111]. The stability of the 'wrapped' enzymes is favorably enhanced, and they remain active [112]. Kataoka et al. [113–115] have shown that C3Ms can be used as carriers for drugs or short pieces of DNA or RNA that need to be delivered at a particular location in the body. The distribution of the drug-loaded micelles in the body is determined mainly by their size and surface properties, rather than by the properties of the incorporated drug molecules. This makes C3Ms very promising drug delivery systems for a wide variety of charged drug molecules.

3.5. Micellar networks

The properties of block-copolymer micelles can be changed drastically if a triblock copolymer with two associating groups per polymer (also called a telechelic polymer) is used instead of a diblock copolymer [116–121]. Triblock copolymers consisting of a water-soluble middle block and two hydrophobic end blocks have been studied extensively. They form so-called flowerlike micelles with a corona that consists of looped middle blocks. When two such flowerlike micelles come together, bridges can be formed between them by polymer chains that have one end block in each micelle. This gives an entropic attraction, which can lead to phase separation into a polymer-rich phase consisting of bridged micelles and a polymer-poor phase consisting of a few flowerlike micelles and free polymers. Above a certain concentration, the whole volume is filled with a transient network consisting of interconnected micelles. The reversible nature of the association makes these networks viscoelastic with a relaxation time that corresponds more or less to the time needed for an end block to dissociate from a micellar core.

Just like hydrophobic interactions can be used to make physical gels, it should also be possible to make physical gels using electrostatic interactions. So far, only very few such gels have been presented. There is some early work on network formation by telechelic polymers with charged end-groups in polymer melts by Register and co-workers [122–124]. They used carboxy-terminated poly(isoprene), sulfonated poly(styrene) or sulfonated poly(urethane) to form ionic clusters with multivalent metal ions, within the polymeric matrix. Similar types of polymers are industrially available, e.g., by DuPont under the trade name of Surlyn®. The first study towards a charge-driven transient network comes from the group of Winnik [125]. They showed an enhanced entanglement strength between positively charged polysaccharide chains by adding negatively charged unimers and micelles. An example of a charge-driven physical gel based on self-assembly comes from the group of Tsitsilianis [126]. They prepared a physical gel by dissolving a polyampholyte in water. The polymer consisted of negatively charged end blocks, which associate with the positively charged middle blocks of the same or other polymers. By doing so, a self-assembled transient network was formed, based on electrostatic interactions.

Recently, we have succeeded in creating a reversible gel based on electrostatic interactions only [127]. This gel features an ABA triblock copolymer in which the A blocks (PSPMA) are negatively charged, and the B block (PEO) is neutral and water soluble. Mixing

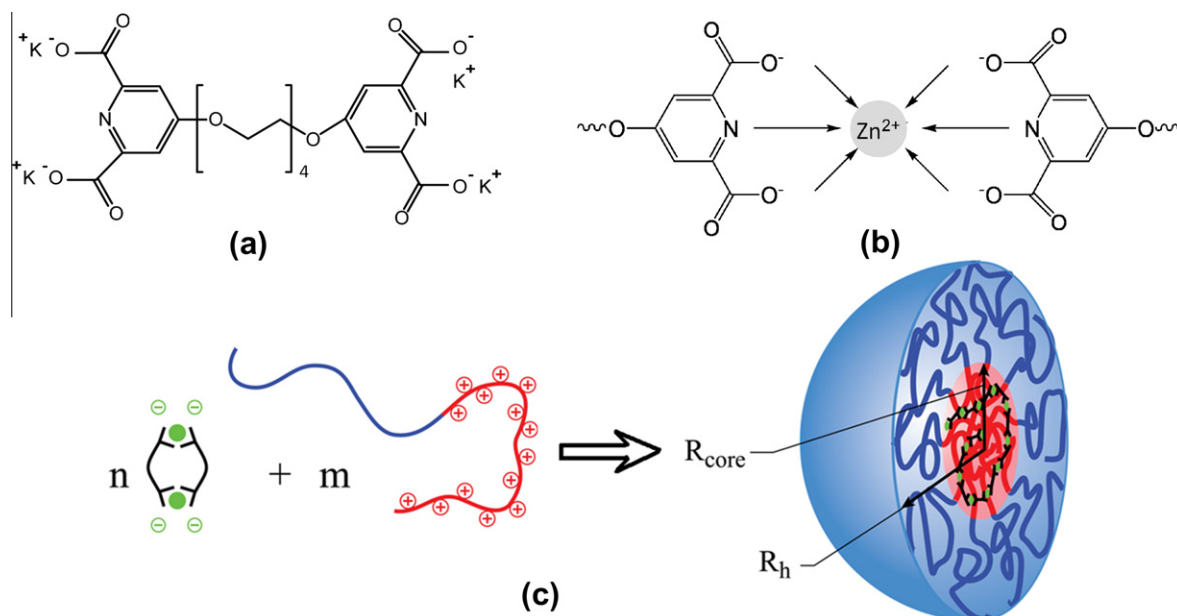


Fig. 12. (a) Structure of a bisligand, which reversibly self-assembles into supramolecular coordination polymers in the presence of metal ions, such as Zn^{2+} (b). The coordination polymer in this case carries a negative charge. (c) A metal-containing C3M formed by association of a coordination polymer with a block copolymer with a cationic block.

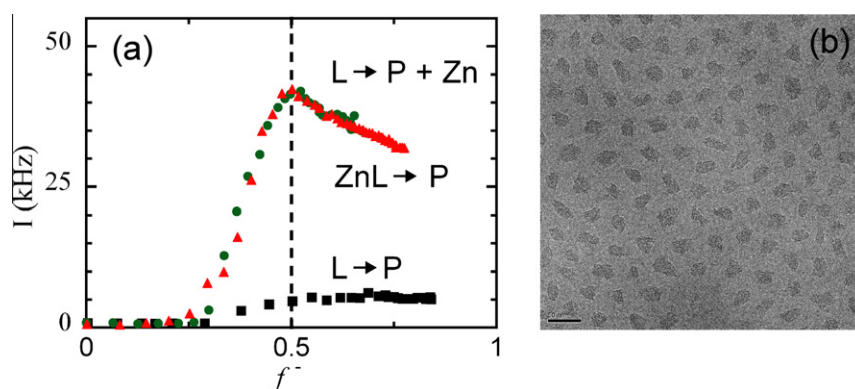


Fig. 13. (a) Light scattering intensity as a function of composition for metal-containing C3Ms. Micelles are formed when coordination polymer (Zn-L) is added to a solution of P2MVP-PEO (P) or when bisligand (L) is added to a solution of P2MVP-PEO and Zn^{2+} (P + Zn). No micelles are formed when bisligand is added to diblock copolymer in the absence of metal. (b) Cryo-TEM picture of metal-containing C3M [5].

this triblock copolymer with a positively charged homopolymer (PAH) leads to the formation of flowerlike micelles at low concentrations (Fig. 14). These micelles are similar to the C3Ms described earlier for combinations of a diblock copolymer and a homopolymer, with the difference that the stabilizing block is now in a looped conformation. Just like the 'classical associative thickeners', the triblock copolymer can have its two charged end blocks in different micellar cores at sufficiently high concentrations. Doing so, the micelles become interconnected and a transient network is formed as shown in Fig. 14. As shown in Fig. 15a, this leads to a very steep increase in the viscosity.

Due to the electrostatic driving force, this charge-driven network is multi-responsive [127]. For example, we showed that the network can be gradually disintegrated by discharging one of the components by increasing the pH. As mentioned before, the charge ratio is an important parameter in polyelectrolyte complex formation. Similar to the diblock/homopolymer systems, we find the strongest driving force for association at charge stoichiometry. Salt concentration is obviously another important parameter to tune the interaction strength between the associating polymers. At high

salt concentrations, association is relatively weak, molecular reorganization is relatively fast and the micelles can quickly equilibrate. As a result, the viscosity decreases strongly upon adding salt to the system (Fig. 15b).

As the salt concentration increases, the aggregation number of the micelles decreases. Since the concentration in these networks is far above the CMC, this implies that all polymeric material are redistributed in more, but smaller micelles, see Fig. 16. Through this process, the average distance between the micelles remains unchanged. This has the remarkable consequence that the storage modulus of such a charge-driven transient network becomes, to a certain extent, independent of salt concentration [128].

Charge-driven transient networks might find application as a new class of aqueous associative thickeners. The ability to precisely tune the interaction strength by varying composition, pH, and salt concentration is a unique feature of these gels. Moreover, the gel is based on the co-assembly of two components, rather than self-assembly of one component. Therefore, one can dissolve one of the components, even in high concentrations, without having any thickening effect. The thickening effect starts only as soon as the

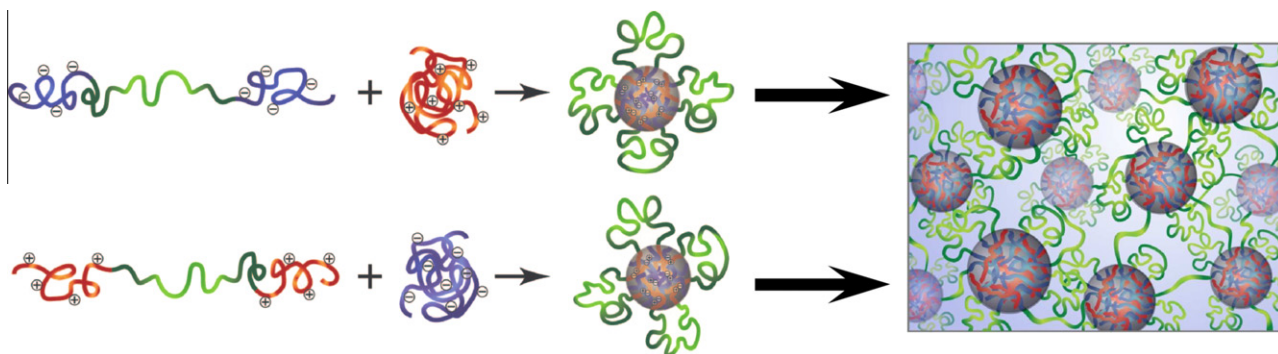


Fig. 14. Schematic representation of physical gel formation based on electrostatic interactions. Triblock copolymers associate into flowerlike micelles upon mixing with oppositely charged homopolymers. At higher concentrations, the micelles become interconnected, forming a transient network.

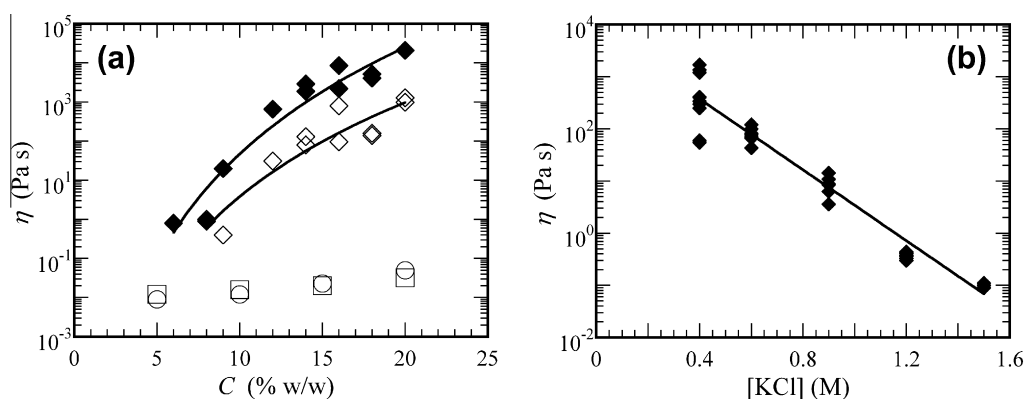


Fig. 15. (a) Viscosity of a C3M network as a function of polymer concentration, for two temperatures: 5 °C (●) and 30 °C (◇). Squares and circles indicate polymer solutions of the two components separately. (b) Viscosity of a C3M network (16%w/w, 20 °C) as a function of [KCl] concentration [127].

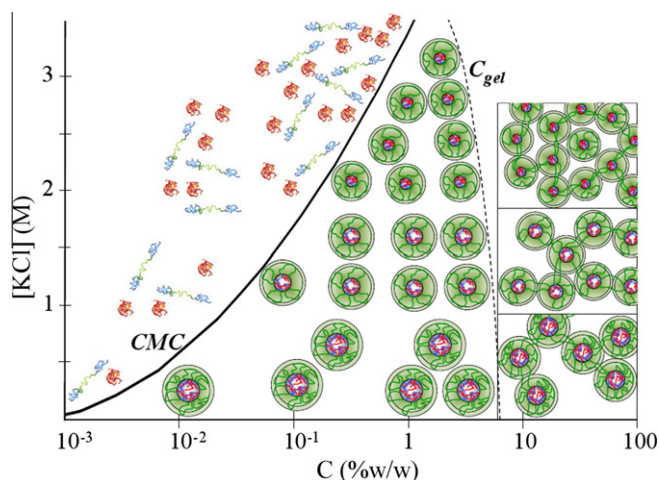


Fig. 16. Illustrated phase diagram for stoichiometric polyelectrolyte complex formation. Total polymer concentration is shown on the horizontal axis, and salt concentration, or driving force for association, is shown on the vertical axis. Below the CMC, only unimers exist in solution. Above the CMC, flowerlike micelles are formed, of which the aggregation number is dependent on the salt concentration. Above the gel concentration, C_{gel} , the flowerlike micelles become interconnected forming a transient network of which the intermicellar spacing is independent of salt concentration.

other component is added to the solution. This characteristic of two-component gels might have significant advantages for stirring and pumping fluids in industry. Another possible application rises from the ability of micelles to carry (bio)active compounds in their

core. Together with the above-described responsiveness of transient networks, this might lead to new ways of controlled release of (bio)active components.

One can think of extending the work described above by combinations of triblock copolymers with equivalent diblock copolymers. The latter should act as network stoppers, adding another parameter to tune the mechanical properties of these charge-driven networks. One can also combine triblock copolymers with oppositely charged diblock copolymers.

Yet another possibility is to mix the triblock copolymer with oppositely charged solid nanoparticles instead of a homopolymer, so that composite gels are obtained. With the possibilities to create colloids of all kinds of shapes, sizes, and magnetic or electrostatic properties, this would open again an entirely new field of research. Such a study is currently carried out at our laboratory.

4. Conclusion and outlook

Polyelectrolyte complexes represent a rather unusual category of polymeric materials, which owe their existence to the association of at least two ingredients, driven by electrostatic attraction between unlike charges. Over the past decade, these complexes, and the nanostructured materials based on them, have become a very active field of research. In particular, thin films made by the layer-by-layer (LBL) method have become very popular, albeit with a strong emphasis on engineering aspects and application rather than on fundamental understanding. In the present paper, we have attempted to have a closer look at such fundamental aspects, paying attention to both static (cohesive energy, interfacial tension) and dynamic (viscoelastic) properties, as well as to theories that

can explain the phase behavior. Some aspects could be clarified, but questions remain: it is not clear what structural factors govern the strength of complexes (chain stiffness, steric effects on proximity of positive and negative charges, chemical nature of the ionic groups), the issue of a glass transition needs further clarification, there is little information on how temperature affects the properties of the complexes, the role of chain length mismatch between the participating polyelectrolytes and the shape of the phase diagram is not entirely clear, and the nature of 'soluble' complexes at off-stoichiometric compositions is not well defined.

Some of the evidence provided shows that stoichiometric polyelectrolyte complexes can be regarded to a large extent as ordinary weakly hydrophobic polymers, with a solvent- and temperature-dependent solubility. Salt-free water is a poor solvent, but salt plays the role that temperature plays for apolar solvents: solubility in water can always be improved by adding salt, and there is a critical salt concentration where phase separation disappears.

Moreover, we discussed colloidal and nanostructured systems, which originate from polyelectrolyte complexes: thin films (LBL), zipper brushes, micelles, and micellar networks. Here, new features appear, such as nanoparticles of broken symmetry (Janus micelles), stuffed micelles, and micelles with metal ions inside, which appear when one polyelectrolyte is replaced by a 'supramolecular coordination polymer' that carries metal ions in its main chain. It is shown that the term 'micelles' is indeed appropriate: a (salt-dependent) CMC can be unambiguously measured. Finally, we looked into the properties of triblock copolymers with two charged end blocks, which can form physical gels with tuneable properties.

Clearly, polyelectrolyte complexes are versatile materials that could possibly be used in a wide range of applications. Most of these applications have not been realized yet, or are in a test phase; medical and pharmaceutical applications would seem to have good chances.

References

- [1] I. Michaeli, J.T.G. Overbeek, M.J. Voorn, *J. Polym. Sci.* 23 (1957) 443.
- [2] B. Philipp, H. Dautzenberg, K.J. Linow, J. Kotz, W. Dawydoff, *Prog. Polym. Sci.* 14 (1989) 91.
- [3] A.F. Thunemann, M. Muller, H. Dautzenberg, J.F.O. Joanny, H. Lowne, in: *Polyelectrolytes with Defined Molecular Architecture II*, 2004, p. 113.
- [4] Y. Cui, R. Pelton, H. Ketelson, *Macromolecules* 41 (2008) 8198.
- [5] Y. Yan, N.A.M. Besseling, A. de Keizer, A.T.M. Marcelis, M. Drechsler, M.A.C. Stuart, *Angew. Chem., Int. Ed.* 46 (2007) 1807.
- [6] C.L. Cooper, P.L. Dubin, A.B. Kayitmazer, S. Turksen, *Curr. Opin. Colloid Interface Sci.* 10 (2005) 52.
- [7] C.G. de Kruif, F. Weinbreck, R. de Vries, *Curr. Opin. Colloid Interface Sci.* 9 (2004) 340.
- [8] K.W. Mattison, I.J. Brittain, P.L. Dubin, *Biotechnol. Prog.* 11 (1995) 632.
- [9] K.W. Mattison, P.L. Dubin, I.J. Brittain, *J. Phys. Chem. B* 102 (1998) 3830.
- [10] C. Schmitt, C. Sanchez, S. Desobry-Banon, J. Hardy, *Crit. Rev. Food Sci. Nutr.* 38 (1998) 689.
- [11] C. Schmitt, C. Sanchez, F. Thomas, J. Hardy, *Food Hydrocolloids* 13 (1999) 483.
- [12] E. Seyrek, P.L. Dubin, C. Tribet, E.A. Gamble, *Biomacromolecules* 4 (2003) 273.
- [13] A. Tsuboi, T. Izumi, M. Hirata, J.L. Xia, P.L. Dubin, E. Kokufuta, *Langmuir* 12 (1996) 6295.
- [14] T. Vinayahan, P.A. Williams, G.O. Phillips, *Biomacromolecules* 11 (2010) 3367.
- [15] F. Weinbreck, R. de Vries, P. Schrooyen, C.G. de Kruif, *Biomacromolecules* 4 (2003) 293.
- [16] M. Antonov, M. Mazzawi, P.L. Dubin, *Biomacromolecules* 11 (2010) 51.
- [17] P.L. Dubin, T.D. Ross, I. Sharma, B.E. Yegerlehner, in: W.L. Hinze, D.W. Armstrong (Eds.), *Ordered Media in Chemical Separations*, American Chemical Society, Washington, DC, 1987, p. 162.
- [18] P.M. Biesheuvel, S. Lindhoud, R. de Vries, M.A. Cohen Stuart, *Langmuir* 22 (2006) 1291.
- [19] V.A. Bloomfield, *Curr. Opin. Struct. Biol.* 6 (1996) 334.
- [20] S.C. De Smedt, J. Demeester, W.E. Hennink, *Pharm. Res.* 17 (2000) 113.
- [21] K. Minagawa, Y. Matsuzawa, K. Yoshikawa, M. Matsumoto, M. Doi, *FEBS Lett.* 295 (1991) 67.
- [22] M. Borkovec, G. Papastavrou, *Curr. Opin. Colloid Interface Sci.* 13 (2008) 429.
- [23] V. Shubin, *J. Colloid Interface Sci.* 191 (1997) 372.
- [24] M.E. Leunissen, C.G. Christova, A.P. Hynninen, C.P. Royall, A.I. Campbell, A. Imhof, M. Dijkstra, R. van Roij, A. van Blaaderen, *Nature* 437 (2005) 235.
- [25] E. Sanz, M.E. Leunissen, A. Fortini, A. van Blaaderen, M. Dijkstra, *J. Phys. Chem. B* 112 (2008) 10861.
- [26] Z.Y. Ou, M. Muthukumar, *J. Chem. Phys.* 124 (2006).
- [27] N. Laugel, C. Betscha, M. Winterhalter, J.C. Voegel, P. Schaaf, V. Ball, *J. Phys. Chem. B* 110 (2006) 19443.
- [28] B. Hof, I.K. Voets, A. de Keizer, M.A.C. Stuart, *Phys. Chem. Chem. Phys.* 8 (2006) 4242.
- [29] A. Kudlay, A.V. Ermoshkin, M. Olvera de la Cruz, *Macromolecules* 37 (2004) 9231.
- [30] A.S. Michaels, R.G. Miekka, *J. Phys. Chem.* 65 (1961) 1765.
- [31] C. Ankerfors, S. Ondaral, L. Wagberg, L. Odberg, *J. Colloid Interface Sci.* 351 (2010) 88.
- [32] J.H. Chen, J.A. Heitmann, M.A. Hubbe, *Colloids Surf., A* 223 (2003) 215.
- [33] A. Naderi, P.M. Claesson, M. Bergstrom, A. Dedinaite, *Colloids Surf., A* 253 (2005) 83.
- [34] H. Dautzenberg, *Macromolecules* 30 (1997) 7810.
- [35] H. Dautzenberg, N. Karibyants, *Macromol. Chem. Phys.* 200 (1999) 118.
- [36] J.T.G. Overbeek, M.J. Voorn, *J. Cell. Comp. Phys.* 49 (1957) 7.
- [37] V.Y. Borue, I.Y. Erukhimovich, *Macromolecules* 23 (1990) 3625.
- [38] M. Castelnovo, J.-F. Joanny, *Langmuir* 16 (2000) 7524.
- [39] A. Kudlay, M. Olvera de la Cruz, *J. Chem. Phys.* 120 (2004) 404.
- [40] M. Castelnovo, J.-F. Joanny, *Eur. Phys. J. E* 6 (2001) 377.
- [41] P.M. Biesheuvel, M.A. Cohen Stuart, *Langmuir* 20 (2004) 4764.
- [42] P.M. Biesheuvel, M.A. Cohen Stuart, *Langmuir* 20 (2004) 2785.
- [43] N. Hoda, R.G. Larson, *Macromolecules* 42 (2009) 8851.
- [44] H. Long, A. Kudlay, G.C. Schatz, *J. Phys. Chem. B* 110 (2006) 2918.
- [45] Y. Hayashi, M. Ullner, P. Linse, *J. Chem. Phys.* 116 (2002) 6836.
- [46] Y. Hayashi, M. Ullner, P. Linse, *J. Phys. Chem. B* 107 (2003) 8198.
- [47] Y. Hayashi, M. Ullner, P. Linse, *J. Phys. Chem. B* 108 (2004) 15266.
- [48] J. Ryden, M. Ullner, P. Linse, *J. Chem. Phys.* 123 (2005).
- [49] A. Veis, C. Aranyi, *J. Phys. Chem.* 64 (1960) 1203.
- [50] A. Veis, *J. Phys. Chem.* 65 (1961) 1798.
- [51] N.N. Oskolkov, Potemkin II, *Macromolecules* 40 (2007) 8423.
- [52] E. Spruijt, A.H. Westphal, J.W. Borst, M.A.C. Stuart, J. van der Gucht, *Macromolecules* 43 (2010) 6476.
- [53] H.G. Bungenberg-de Jong, H.R. Kruyt, *Proc. Sect. Sci. Koninklijke Nederlandse Akademie van Wetenschappen* 32 (1929) 849.
- [54] R. Chollakup, W. Smitthipong, C.D. Eisenbach, M. Tirrell, *Macromolecules* 43 (2010) 2518.
- [55] M.A. Cohen Stuart, R. de Vries, J. Lyklema, in: J. Lyklema (Ed.), *Fundamentals of Colloid and Interface Science*, vol. 5, Academic Press, London, 1991.
- [56] E. Spruijt, M.A. Cohen Stuart, J. van der Gucht, *Macromolecules* 43 (2010) 1543.
- [57] E. Spruijt, J. Sprakel, M.A.C. Stuart, J. van der Gucht, *Soft Matter* 6 (2010) 172.
- [58] J. Sprakel, N.A.M. Besseling, F.A.M. Leermakers, M.A.C. Stuart, *Phys. Rev. Lett.* 99 (2007) 104504.
- [59] F. Weinbreck, R.H.W. Wientjes, H. Nieuwenhuijs, G.W. Robijn, C.G. De Kruif, *J. Rheol.* 48 (2004) 1215.
- [60] E. Spruijt, J. Sprakel, M. Lemmers, M.A.C. Stuart, J. van der Gucht, *Phys. Rev. Lett.* 105 (2010), article no: 208301.
- [61] D. Kovacevic, S. van der Burgh, A. de Keizer, M.A.C. Stuart, *Langmuir* 18 (2002) 5607.
- [62] G. Decher, J.D. Hong, J. Schmitt, *Thin Solid Films* 210 (1992) 831.
- [63] G. Decher, J. Lvov, J. Schmitt, *Thin Solid Films* 244 (1994) 772.
- [64] M. Losche, J. Schmitt, G. Decher, W.G. Bouwman, K. Kjaer, *Macromolecules* 31 (1998) 8893.
- [65] J. Schmitt, T. Grunewald, G. Decher, P.S. Pershan, K. Kjaer, M. Losche, *Macromolecules* 26 (1993) 7058.
- [66] P. Bertrand, A. Jonas, A. Laschewsky, R. Legras, *Macromol. Rapid Commun.* 21 (2000) 319.
- [67] G. Decher, *Science* 277 (1997) 1232.
- [68] S.T. Dubas, J.B. Schlenoff, *Macromolecules* 32 (1999) 8153.
- [69] Y.M. Guo, W. Geng, J.Q. Sun, *Langmuir* 25 (2009) 1004.
- [70] J. Lvov, G. Decher, H. Mohwald, *Langmuir* 9 (1993) 481.
- [71] G.B. Sukhorukov, E. Donath, S. Davis, H. Lichtenfeld, F. Caruso, V.I. Popov, H. Mohwald, *Polym. Adv. Technol.* 9 (1998) 759.
- [72] P. Laval, F. Boulmedais, V. Ball, J. Mutterer, P. Schaaf, J.C. Voegel, *J. Membr. Sci.* 253 (2005) 49.
- [73] A.A. Mamedov, N.A. Kotov, *Langmuir* 16 (2000) 5530.
- [74] F. Caruso, *Chem. -Eur. J.* 6 (2000) 413.
- [75] F. Caruso, R.A. Caruso, H. Mohwald, *Science* 282 (1998) 1111.
- [76] E. Donath, G.B. Sukhorukov, F. Caruso, S.A. Davis, H. Mohwald, *Angew. Chem., Int. Ed.* 37 (1998) 2202.
- [77] C.S. Peyratout, L. Dahne, *Angew. Chem., Int. Ed.* 43 (2004) 3762.
- [78] P.M. Biesheuvel, T. Mauser, G.B. Sukhorukov, H. Mohwald, *Macromolecules* 39 (2006) 8480.
- [79] T. Mauser, C. Dejgnet, G.B. Sukhorukov, *Macromol. Rapid Commun.* 25 (2004) 1781.
- [80] P. Laval, C. Picart, J. Mutterer, C. Gergely, H. Reiss, J.C. Voegel, B. Senger, P. Schaaf, *J. Phys. Chem. B* 108 (2004) 635.
- [81] C. Picart, J. Mutterer, L. Richert, Y. Luo, G.D. Prestwich, P. Schaaf, J.C. Voegel, P. Laval, *Proc. Natl. Acad. Sci. U. S. A.* 99 (2002) 12531.
- [82] P. Laval, V. Vivet, N. Jessel, G. Decher, J.C. Voegel, P.J. Mesini, P. Schaaf, *Macromolecules* 37 (2004) 1159.
- [83] L. Jourdainne, S. Lecuyer, Y. Arntz, C. Picart, P. Schaaf, B. Senger, J.C. Voegel, P. Laval, T. Charitat, *Langmuir* 24 (2008) 7842.

- [84] B. Hofs, A. Brzozowska, A. de Keizer, W. Norde, M.A.C. Stuart, J. Colloid Interface Sci. 325 (2008) 309.
- [85] W.M. de Vos, J.M. Kleijn, A. de Keizer, M.A. Cohen Stuart, Angew. Chem., Int. Ed. 48 (2009) 5369.
- [86] W.M. de Vos, G. Meijer, A. de Keizer, M.A.C. Stuart, J.M. Kleijn, Soft Matter 6 (2010) 2499.
- [87] V.A. Kabanov, A.B. Zevin, Pure Appl. Chem. 56 (1984) 343.
- [88] E. Tsuchida, J. Macromol. Sci., Part A: Pure Appl. Chem. A31 (1994) 1.
- [89] M. Muller, T. Reihls, W. Ouyang, Langmuir 21 (2005) 465.
- [90] A. Harada, K. Kataoka, Macromolecules 28 (1995) 5294.
- [91] A.V. Kabanov, T.K. Bronich, V.A. Kabanov, K. Yu, A. Eisenberg, Macromolecules 29 (1996) 6797.
- [92] M.A. Cohen Stuart, N.A.M. Besseling, R.G. Fokkink, Langmuir 14 (1998) 6846.
- [93] J.F. Gohy, S.K. Varshney, S. Antoun, R. Jerome, Macromolecules 33 (2000) 9298.
- [94] D.V. Pergushov, E.V. Remizova, J. Feldthausen, A.B. Zevin, A.H.E. Muller, V.A. Kabanov, J. Phys. Chem. B 107 (2003) 8093.
- [95] I.K. Voets, A. de Keizer, M.A. Cohen Stuart, Adv. Colloid Interface Sci. 147–148 (2009) 300.
- [96] S. van der Burgh, A. de Keizer, M.A.C. Stuart, Langmuir 20 (2004) 1073.
- [97] A. Harada, K. Kataoka, Science 283 (1999) 65.
- [98] J. Sprakel, F.A.M. Leermakers, M.A.C. Stuart, N.A.M. Besseling, Phys. Chem. Chem. Phys. 10 (2008) 5308.
- [99] S.V. Solomatin, T.K. Bronich, T.W. Bargar, A. Eisenberg, V.A. Kabanov, A.V. Kabanov, Langmuir 19 (2003) 8069.
- [100] J.Y. Wang, A. de Keizer, R. Fokkink, Y. Yan, M.A.C. Stuart, J. van der Gucht, J. Phys. Chem. B 114 (2010) 8313.
- [101] Y. Yan, A. de Keizer, M.A.C. Stuart, M. Drechsler, N.A.M. Besseling, J. Phys. Chem. B 112 (2008) 10908.
- [102] I.K. Voets, S. van der Burgh, B. Farago, R. Fokkink, D. Kovacevic, T. Hellweg, A. de Keizer, M.A. Cohen Stuart, Macromolecules 40 (2007) 8476.
- [103] B. Hofs, A.d. Keizer, S.v.d. Burgh, F.A.M. Leermakers, M.A.C. Stuart, P.-E. Millard, A.H.E. Muller, Soft Matter 4 (2008) 1473.
- [104] M. Charlaganov, O.V. Borisov, F.A.M. Leermakers, Macromolecules 41 (2008) 3668.
- [105] I.K. Voets, A. de Keizer, P. de Waard, P.M. Frederik, P.H.H. Bomans, H. Schmalz, A. Walther, S.M. King, F.A.M. Leermakers, M.A. Cohen Stuart, Angew. Chem., Int. Ed. 45 (2006) 6673.
- [106] I.K. Voets, R. Fokkink, T. Hellweg, S.M. King, P. de Waard, A. de Keizer, M.A.C. Stuart, Soft Matter 5 (2009) 999.
- [107] I.K. Voets, P.M. Moll, A. Aqil, C. Jerome, C. Detrembleur, P. de Waard, A. de Keizer, M.A.C. Stuart, J. Phys. Chem. B 112 (2008) 10833.
- [108] T. Vermonden, J. van der Gucht, P. de Waard, A.T.M. Marcelis, N.A.M. Besseling, E.J.R. Sudholter, G.J. Fleer, M.A.C. Stuart, Macromolecules 36 (2003) 7035.
- [109] Y. Yan, A. de Keizer, M.A. Cohen Stuart, M. Drechsler, N.A.M. Besseling, J. Phys. Chem. B 112 (2008) 10908.
- [110] A. Harada, K. Kataoka, Macromolecules 31 (1998) 288.
- [111] S. Lindhoud, R. de Vries, W. Norde, M.A. Cohen Stuart, Biomacromolecules 8 (2007) 2219.
- [112] S. Lindhoud, W. Norde, M.A.C. Stuart, Langmuir 26 (2010) 9802.
- [113] R. Ideta, Y. Yanagi, Y. Tamaki, F. Tasaka, A. Harada, K. Kataoka, FEBS Lett. 557 (2004) 21.
- [114] Y. Kakizawa, K. Kataoka, Adv. Drug Delivery Rev. 54 (2002) 203.
- [115] K. Kataoka, T. Matsumoto, M. Yokoyama, T. Okano, Y. Sakurai, S. Fukushima, K. Okamoto, G.S. Kwon, J. Controlled Release 64 (2000) 143.
- [116] T. Annable, R. Buscall, R. Ettelaie, D. Whittlestone, J. Rheol. 37 (1993) 695.
- [117] R.D. Jenkins, D.R. Bassett, C.A. Silebi, M.S. El-Aasser, J. Appl. Polym. Sci. 58 (1995) 209.
- [118] R.D. Jenkins, C.A. Silebi, M.S. El-Asser, ACS Symp. Ser. 462 (1991) 222.
- [119] X.X. Meng, W.B. Russel, J. Rheol. 50 (2006) 189.
- [120] J. Sprakel, N. Besseling, M. Cohen Stuart, F. Leermakers, Eur. Phys. J. E 25 (2008) 163.
- [121] J. Sprakel, E. Spruijt, M.A. Cohen Stuart, N.A.M. Besseling, M.P. Lettinga, J. van der Gucht, Soft Matter 4 (2008) 1696.
- [122] Y.S. Ding, S.R. Hubbard, K.O. Hodgson, R.A. Register, S.L. Cooper, Macromolecules 21 (1988) 1698.
- [123] R.A. Register, M. Foucart, R. Jerome, Y.S. Ding, S.L. Cooper, Macromolecules 21 (1988) 1009.
- [124] R.A. Register, G. Pruckmayr, S.L. Cooper, Macromolecules 23 (1990) 3023.
- [125] R.C.W. Liu, Y. Morishima, F.M. Winnik, Polym. J. 34 (2002) 340.
- [126] F. Bossard, V. Sfika, C. Tsitsilianis, Macromolecules 37 (2004) 3899.
- [127] M. Lemmers, J. Sprakel, I.K. Voets, J. van der Gucht, M.A. Cohen Stuart, Angew. Chem., Int. Ed. 49 (2010) 708.
- [128] M. Lemmers, I.K. Voets, M.A. Cohen Stuart, J. van der Gucht, Soft Matter 7 (2011) 1378.